Contractile Properties of Skeletal Muscles in Hypertrophic Cardiomyopathy.

A thesis submitted to McGill University in partial fulfillment of the requirements of the degree of Master of Science

Department of Kinesiology and Physical Education
Faculty of Education
McGill University
Montreal, Quebec, Canada

October, 2019

TABLE OF CONTENTS

Acknowledgements

First and foremost, I would like to express my sincere gratitude to my supervisor Dr. Dilson E. Rassier for his continuous support over the course of my MSc studies and research in the Muscle Physiology and Biophysics laboratory. His guidance, enthusiasm and expertise has played an immense role in bringing this thesis to fruition. I could not have imagined a better advisor and mentor throughout this journey of my MSc studies.

Secondly, I would like to express my appreciation to the Department of Kinesiology and Physical Education (Graduate Excellence Award), Natural Science and Engineering Research Council of Canada (NSERC), and McGill University (International Tuition Support Bursary) for their financial support. Thirdly, I would like thank Dr. Oleg S. Matusovsky, Dr. Yu-Shu Cheng, Daren Elkrief and other members of the Muscle Physiology and Biophysics lab including Dr. Felipe de Souza Leite, Dr. Malin Persson, Ricarda Haeger, Caitlin MacEachen, Andrea Mendoza, Anju Philip and Giulia Del Guercio Green for their encouragement over the course of this degree.

Last but not least, I am grateful to my family and friends for their continuous support of my academic endeavors.

Contribution of Authors

The primary author of this thesis was Md Rezuanul Haque Saikat, who conducted experiments, data collection, data analysis, and manuscript preparation. Training for the experiment systems was done by Dr. Oleg S. Matusovsky and Dr. Yu-Shu Cheng. The research design, data analysis and preparation of the manuscript was performed under the supervision of Dr. Dilson E. Rassier.

List of Figures

0.2276 ± 0.0271) and soleus (TG+ 0.1983 ± 0.0079) muscles were significantly lower compared to WT myosin diaphragm (WT 0.5489 ± 0.0132) and soleus (WT 0.2984 ± 0.0044) respectively. (B) The Mg^{2+}ATPase activity for the TG+ HMM of the diaphragm (TG+ 0.081 ± 0.0060) and soleus (TG+ 0.0203 ± 0.0037) muscles were also significantly lower compared to the WT HMM diaphragm (WT 0.1838 ± 0.0044) and soleus (WT 0.099 ± 0.0028) respectively, which follows the similar pattern observed with the myosin preparations. Meanwhile, the psoas muscle does not show any differences when myosin was used (P=0.768) or HMM (P=0.245). 53

List of Tables

Abstract

Rationale: There is evidence of skeletal muscles weakness in patients with hypertrophic cardiomyopathy (HCM), but the mechanism behind muscle weakness has yet to be revealed at the molecular level.

Objective: To investigate the potential mechanisms which lead to muscle weakness in the diaphragm, soleus and psoas muscles in a rabbit model of HCM that presents a R403Q missense mutation in β-myosin heavy chain (β-MyHC), responsible for familial HCM.

Hypothesis: The contractile proteins of diaphragm and soleus muscle taken from transgenic (TG+) rabbit with a R403Q mutation in the cardiac β-MyHC will produce less ATPase activity and velocity of actin sliding over myosin molecules when compared to wild type (WT) muscles, given that cardiac β-MyHC expresses in cardiac and slow skeletal muscles. There will be no differences in the velocity and ATPase activity in the psoas muscle between the two groups.

Methods: Two different types of experiments were performed on purified myosin and heavy meromyosin (HMM) of the diaphragm, soleus, and psoas muscles of WT and TG+ rabbits to assess actin sliding velocity and ATPase activity: in-vitro motility assay (IVMA) and actin activated ATPase assay.

Results: The TG+ HMM from diaphragm and soleus muscles produced actin sliding velocities that were 16% and 22% lower than WT HMM, respectively. The ATPase activity of diaphragm and soleus TG+ myosin and HMM were also significantly lower than WT samples. However, there was no difference in the actin velocity and ATPase activity for the psoas muscle.

Conclusion: HCM changes the contractile properties of the diaphragm and soleus muscles at the molecular level, leading to a lower velocity of myosin-induced actin motility and lower ATPase activity.

Résumé

Justification: Il existe des signes de faiblesse au niveau des muscles squelettiques chez les patients atteints de cardiomyopathie hypertrophique (CMH), mais le mécanisme derrière la faiblesse musculaire n'a pas encore été révélé au niveau moléculaire.

Objectifs: Pour étudier les mécanismes potentiels qui contribuent à la faiblesse musculaire du diaphragme, du soléus et du psoas dans un modèle de lapin de CHM présentant une mutation faux-sens R403Q dans la chaîne lourde de la β-myosine (β-MyHC) qui a été utilisée.

Hypothèse: Les protéines contractiles du diaphragme et du soleus extraites des lapins transgéniques (TG+), porteurs d'une mutation R403Q dans le bêta-MyHC cardiaque, présentaient moins d'activité ATPase et de vitesse d'actine glissant sur les molécules de myosine par rapport aux muscles de type sauvage (WT), suggérant que le β-MyHC cardiaque s'exprime dans les muscles cardiaques et squelettiques lents. Il n'y aura pas de différence dans la vitesse et dans l'activité ATPase du muscle psoas entre les deux groupes.

Mèthodes: Deux types d'expériences ont été effectuées sur la myosine purifiée et la méromyosine lourde (HMM) du diaphragme, du soléus et du psoas de WT et TG + chez des lapins afin d'évaluer la vitesse de glissement de l'actine et l'activité de l'ATPase: test de mobilité in vitro (IVMA) et ATPase de myosine activée par l'actine.

Rèsultats: Les TG + HMM des muscles du diaphragme et du soléus ont produit des vitesses de glissement de l'actine respectivement 16% et 22% inférieures à celles du WT HMM. L'activité ATPase du diaphragme et du soléus TG + myosine et HMM était également significativement inférieure à celle des échantillons WT. Cependant, il n'y a aucune différence par rapport a la vitesse d'actine et l'activité de l'ATPase pour le psoas musculaire.

Conclusion: La CHM modifie les propriétés contractiles des muscles du diaphragme et du soléus au niveau moléculaire, ce qui cause une diminution de la vitesse de la motilité de l'actine induite par la myosine et de l'activité de l'ATPase.

CHAPTER 1 - LITARATURE REVIEW

1. Introduction

The human body is complex, and yet composed of orderly arranged biological systems. The musculoskeletal system is composed of bones, muscles and connective tissues with the main function of movement of the body. The respiratory and circulatory systems extract oxygen and circulate blood to the musculoskeletal system in order to maintain body homeostasis.

The diaphragm and abdomen work in a coordinated fashion during respiration and during cardiac function to directly and indirectly control the respiratory muscle activity (McNally & Goldstein, 2012). All the physiological systems work individually, but are interconnected to perform multiple functions in the body. The autonomous cardiac conducting system is also connected to these systems (Kasper, 2015), and counts with specialized muscle cells that help to maintain the heart beating cycle. All these muscle functions can be disrupted due to the presence of genetic or acquired cardiac abnormalities, which alter the heart physiology as well as other associated systems and comorbidities.

Cardiomyopathy is a myocardial disease that usually exhibits ventricular hypertrophy associated with mechanical and/or electrical dysfunction of the heart. It can lead to cardiac dysfunctions, such as arrhythmia, hemodynamic deterioration, congestive heart failure and sudden cardiac arrest. However, the complication of this disease is not limited to the cardiovascular system. It can affect the respiratory and musculoskeletal systems which increases the load on the diaphragm muscle, thus causing a form of skeletal myopathy (Fananapazir, Dalakas, Cyran, Cohn, & Epstein, 1993; Howell et al., 1995; Mancini, Henson, LaManca, & Levine, 1992). Additionally, cardiomyopathy patients exhibit histological changes including skeletal muscle atrophy and fiber type alterations (Cuda, Fananapazir, Zhu, Sellers, & Epstein, 1993; Howell et al., 1995; Hughes et al., 1999; Kemp et al., 1996; Lecarpentier et al., 1998). These secondary changes in the respiratory

and limb musculature caused by this disease can limit the normal activity of the body (De Sousa et al., 2001; Mancini et al., 1992). Identifying this type of muscle dysfunction is one of the key clinical findings in congestive cardiac failure (Belus et al., 2008).

It is well accepted that loss of cardiac function leads to respiratory muscle weakness resulting in dyspnea upon exertion in cardiomyopathy patients. However, multiple studies on diaphragm performance have shown that other factors such as genetic adaptation can also be associated with altering the respiratory response (Dominguez & Howell, 2003; Eddinger & Moss, 1987; Eddinger, Moss, & Cassens, 1985; Geiger, Cody, Macken, & Sieck, 2000; Howell et al., 1995; Lecarpentier et al., 1998; Lecarpentier, Coirault, Langeron, et al., 1999). The majority of studies investigating cardiomyopathy have been performed using respiratory muscles from mouse models, which do not exhibit the same phenotypic characteristics as human cardiomyopathy patients (Hasenfuss, 1998). Understanding the entire pathophysiology of respiratory adaptation in HCM causing congestive cardiac failure is challenging - for instance, despite a decreased diaphragm function, there are studies that observe an increase in force due to the presence of cardiomyopathy mutations, such as the MYH7 mutation (P. A. Ribeiro et al., 2013; Tikunov, Levine, & Mancini, 1997; van Hees et al., 2007).

The MYH7 gene mutation causing the cardiomyopathy is also responsible for skeletal muscle diseases like the Myosin Storage Myopathy and the Laing Distal Myopathy (Lamont et al., 2014). Few clinical and experimental studies have explored the pathophysiology of skeletal muscles performance in cardiomyopathy, despite the fact that cardiac β-MyHC is expressed in both cardiac and slow skeletal muscles (Tajsharghi & Fyhr, 2008). One major limitation in these studies has been the choice of disease model. These studies have used mice. The myosin isoform of mice is not similar to the myosin isoform of humans, and it does not relate to human

cardiomyopathy models. Therefore, the present investigation was undertaken to examine the molecular mechanism behind the alteration of skeletal muscle function in HCM through the use of an appropriate animal model, which will be described later in this thesis.

2. Skeletal muscle

The skeletal muscle consists of long, cylindrical multinucleated muscle fibers. Each fiber contains filament bundles called myofibrils, which run parallel along the axis of the fiber. The functional subunit of the contractile apparatus is the sarcomere, which is approximately 2.5μm long in resting conditions. The sarcomere boundaries are defined between two Z-discs, structures which repeat along the myofiber, along with repeating regions called the I-band, A-band, M-line and H zone (Figure 1).

The Z-disc is the connecting region for thick and thin filaments. The thin filaments contain actin-binding proteins, α-actinin, titin and nebulin, responsible for maintaining sarcomere structure (Luther, 2009). The diameter of the Z-disc depends on the muscle fibers type and species related to α-actinin content (Luther, 2009). A titin filament is a giant protein composed of a repeating coiled-coil structure extending from the M-line, or the middle of the sarcomere, to the Z-band (Bang et al., 2001). Nebulin, controls the length of the thin filaments (Labeit, Ottenheijm, & Granzier, 2011). The thick filaments occupy the middle area of sarcomere and are divided by the M-line, which is located within the H-zone. The H-zone contains only the rod-like portion of thick filaments, but no thin filaments (Figure 1).

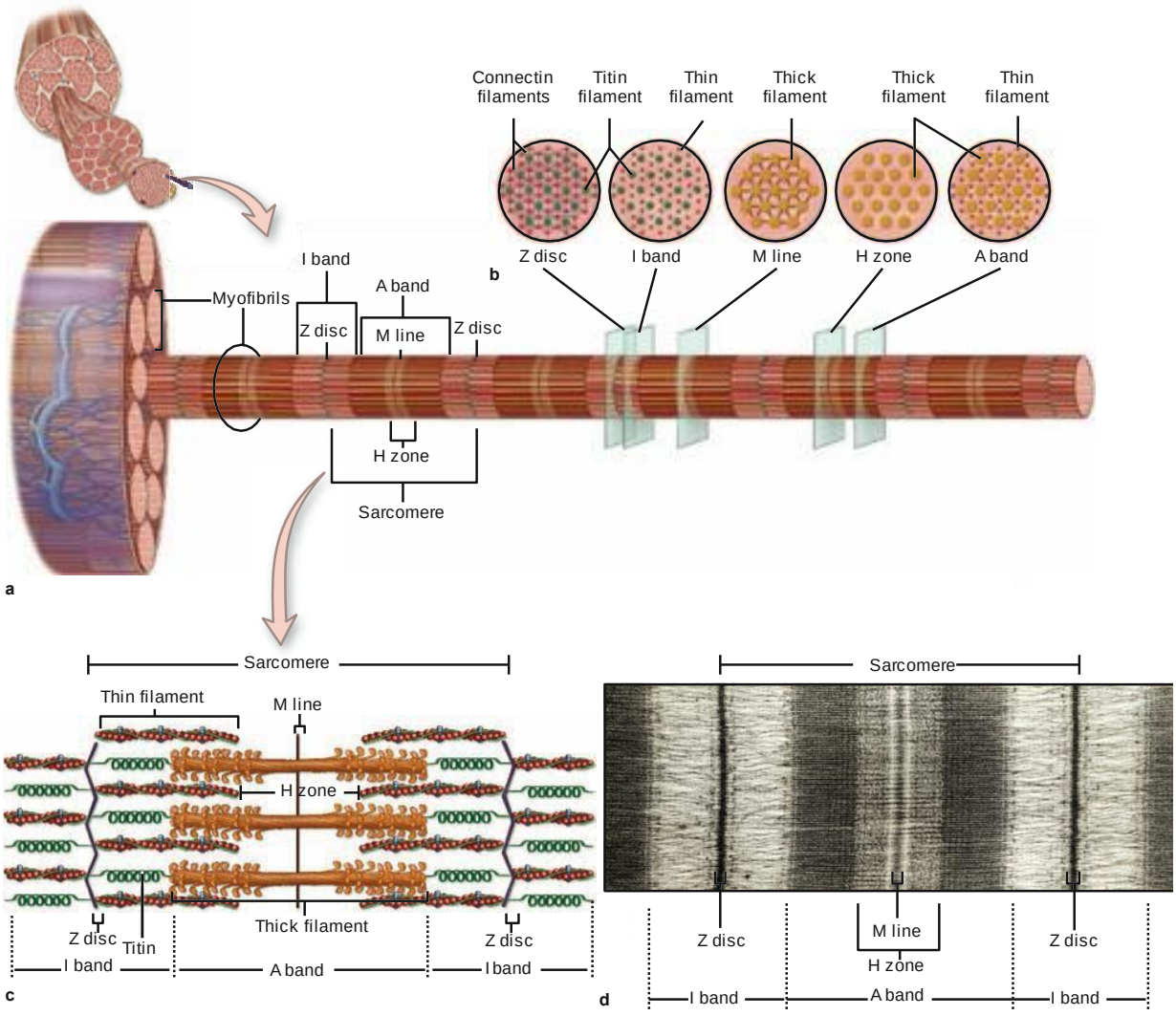

Figure 1. Schematic presentation of a myofibril and a sarcomere (Adapted from Mescher & Junqueira, 2016). (a) The muscle fiber contains several parallel bundles of myofibrils. (b) Each myofibril contains series of sarcomeres which consists of thick and thin filaments that overlap in an organized way. (c) Thin and thick filaments are actin and myosin bundles, respectively. Actin filaments are bound to α-actinin in the Z-disc at one end. Myosin spans the whole A-band. The I-band is located between the A-bands, which contains mostly thin filaments. (e) The structural organization of the sarcomere as observed in light microscopy.

2.1 Mechanism of contraction

The mechanism of muscle contraction was unknown until the sliding filament hypothesis was proposed by Huxley in the mid 20th century (A. F. Huxley, 1957). According to this model, the force of muscle contraction is generated when thick and thin filaments slide past each other. The sliding of filaments is driven by a cyclic attachment and detachment between myosin cross-bridges and actin. The myosin head, or myosin subfragment S1 goes through a so-called power stroke while interacting with actin filaments, producing muscle contraction and force (H. E. Huxley, 1969; Lymn & Taylor, 1971). A rotating of the myosin tail acts as a lever arm which amplifies the conformational changes in the catalytic domain of myosin head (Holmes & Geeves, 2000; A. F. Huxley, 2000; Rayment et al., 1993).

2.1.1 Actin and myosin

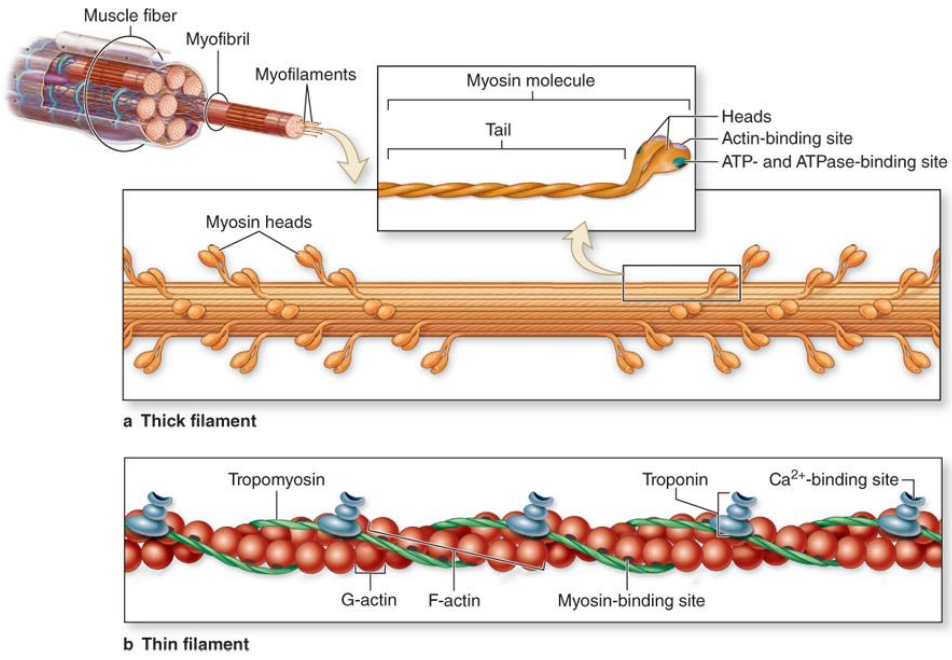

Figure 2. Myofilaments consist of thick and thin filaments (Adapted from Mescher & Junqueira, 2016). (a) A thick filament contains 200 to 500 molecules of myosin. Each of the myosin molecules

has a long tail and head domain contains the actin-binding site and ATP binding site. (b) A thin filament consists mostly of F actin, tropomyosin, and troponin.

The sarcomere is the basic structural unit of striated muscles and is mainly composed of thin and thick filaments. Thin filaments are composed of F actin, troponin and the tropomyosin complex, which regulates the actomyosin interaction by controlling calcium-induced activation of the contractile system (Fatkin & Graham, 2002). Actin filaments are thin helical shaped proteins, approximately 8nm wide and 1.0μm long (Mescher & Junqueira, 2016). There are two forms of actin: free monomer globular shaped G actin and the polymer formed with G actin; the filamentous F actin (Figure 2). Actin participates in cellular motility, and it contributes to cell integrity, cell polarity and transcriptional regulation.

The muscle contraction depends on the interaction of myosin with F actin (Szent-Gyorgyi, 2004). In mammals, actin is expressed as three different isoforms: α-actin, β-actin and γ-actin, although there are only a few amino acid differences between them (Herman, 1993).

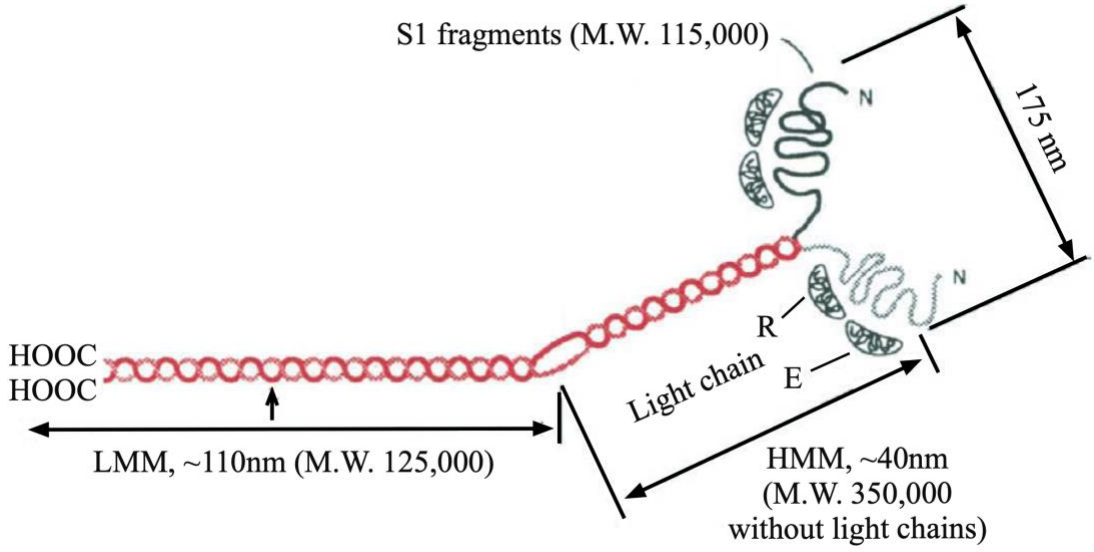

Figure 3. Schematic representation of the myosin head. Light meromyosin (LMM) is a coiled-coil helical structure, approximately 2nm thick. Heavy meromyosin (HMM) is a partially coiled-coil

structure which contains subfragment-1 (S1), regulatory light chain (R) and essential light chain (E) (Adapted from Bhagavan, 2002).

The main component of the thick filament is myosin, which is 1.6μm long and 15nm wide. Thick filaments are located in the middle area of the sarcomere, predominantly in the A-band. Myosin is composed of two identical heavy chains, a pair of essential light chains (ELC), a pair of regulatory light chain (RLC), one N-terminal motor domain and one α-helical coiled-coil dimer (Figure 3). Heavy meromyosin (HMM) and light meromyosin (LMM) can be fragmented by enzymatic cleavage of myosin. Each head of the MyHC contains the actin-binding site and the ATPase binding site. Additionally, other proteins like myosin binding protein C and titin are also associated with thick filaments and contribute to contractile regulation (Rayment, 1996; Tang et al., 2016).

HMM plays a key role while interacting with actin filaments during ATPase activity (Barouch & Moos, 1971; Dancker, 1975). HMM can be divided into two subfragments: subfragment 1 (S1) and subfragment 2 (S2). The S1 fragment is composed of two globular-shaped myosin heads responsible for binding with actin (Figure 3). The upper part of the myosin tail connecting the two meromyosin fragments can be referred to as S2 fragment (Figure 3). Each myosin head has a motor domain and two myosin light chains (MLCs). The MLCs can be divided into an essential light chain and a regulatory light chain.

2.1.2 Myosin ATPase cycle

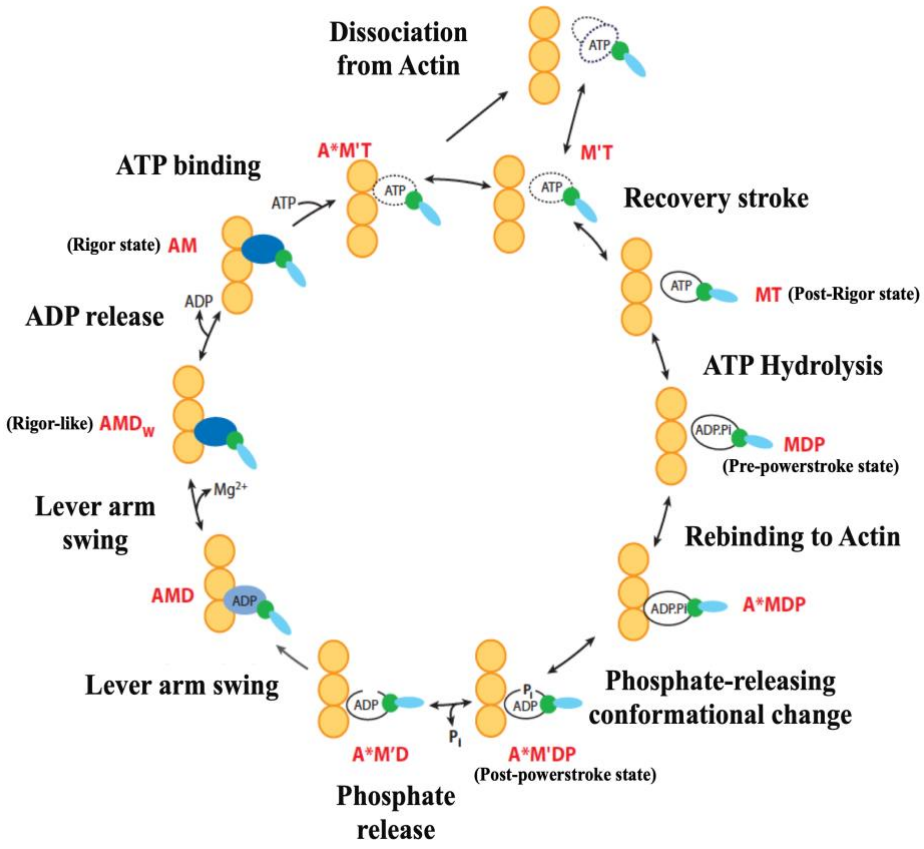

Figure 4. A simplified model of the myosin ATPase cross-bridge cycle (Adapted from Sweeney & Houdusse, 2010). A is actin, M is myosin, D is adenosine diphosphate (ADP), T is adenosine triphosphate (ATP), P is inorganic phosphate.

The myosin-actin interaction steps are collectively known as the 'power stroke cycle'. The first stage of the cycle begins with the actomyosin complex in a rigor state-without ATP. Next, ATP binding to the myosin opens a cleft in the molecule causing myosin to detach from actin. ATP binding decreases the myosin affinity for actin at this (AM) stage. Following, ATP is hydrolyzed into ADP. Pi and myosin are allowed to reattach to actin during the M state. After release of organic phosphate (Pi) and the ADP, the power stroke can occur, and myosin transforms the chemical energy liberated from ATP hydrolysis into mechanical work (Figure 4).

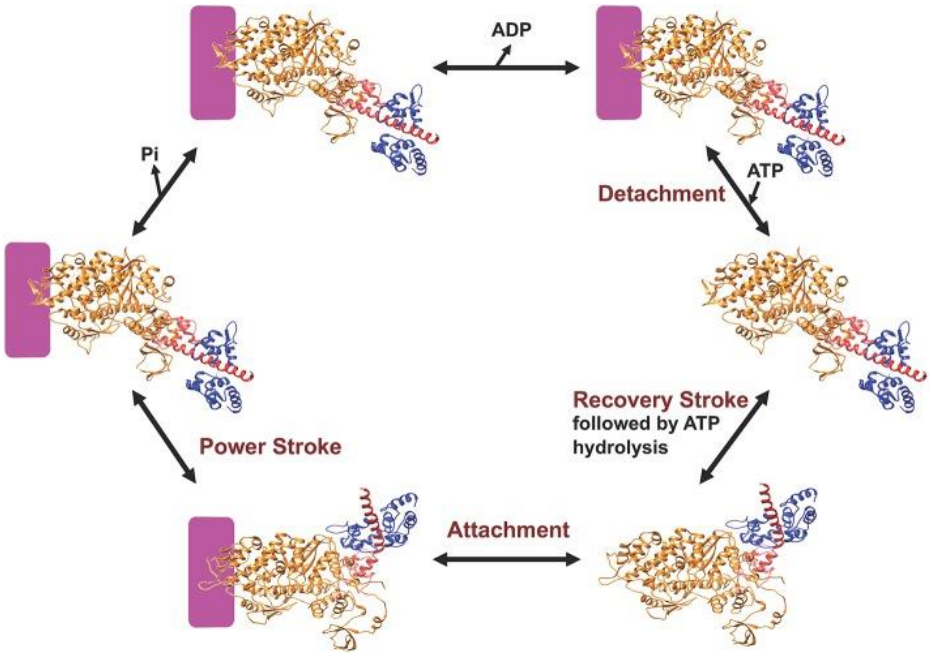

Figure 5. The ribbon diagram of the myosin ATPase cycle in different structural stages (Adapted from Tang et al., 2016). The lever arm is shown in red, the light chain is shown in blue and the actin is shown as the purple box.

In the initial stage, the myosin head is tightly bound and locked in a 45° configuration with the tail (Figure 5). At this stage, the long cleft of the ATP binding site is closed. ATP binds to myosin by opening the cleft, causing a conformational change in the actin-binding region, after which ATP is hydrolyzed into ADP and Pi. Only one molecule of ATP is hydrolyzed during this cross-bridge cycle. Actin weakly binds with a myosin-ADP-Pi complex which forms the pre-power state of the lever arm (Tang et al., 2016). Then, myosin binds strongly to actin to reverse the conformational changes by releasing the Pi, followed by release of ADP. This last step generates the force with the pivotal movement of the lever arm, i.e., the power stroke. The structural transition of the myosin head led by the lever arm rotation determines the actin-binding

affinity. Thus, both the myosin head and the α-helical tail contribute to the displacement of actin. (Fatkin & Graham, 2002).

2.1.3 Regulation of contraction

The troponin-tropomyosin complex is the Ca^{2+}-dependent regulatory system that controls actomyosin interaction in skeletal and cardiac muscles. Tropomyosin is a coiled-coil parallel dimer that is 40nm long, and it is situated in the groove of actin filaments in head to tail orientation (Figure 6) (Khaitlina, 2015). The troponin complex is composed of three subunits: troponin T (TnT), troponin I (TnI) and troponin C (TnC). The troponin complex is located on top of the tropomyosin filament. TnT is the subunit which facilitates interaction between troponin and tropomyosin. In relaxed muscle, TnI binds to actin, inhibiting the actin-binding site from interacting with myosin. During contraction, Ca^{2+} binds to TnC, which weakens the TnI inhibition and the actin-tropomyosin interaction. This causes a conformational change in the troponin complex, and an azimuthal movement of tropomyosin away from its initial position that opens the actin-binding site for myosin, allowing for cross-bridge formation (Fatkin & Graham, 2002).

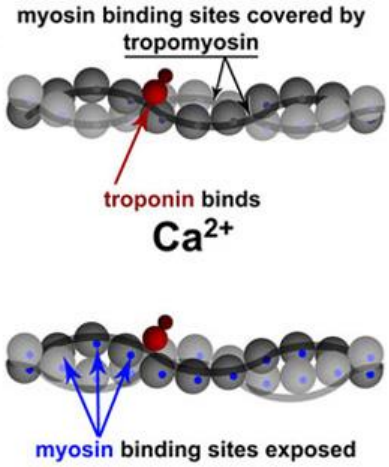

Figure 6. Simplified schematic view of actin backbones along with troponin and tropomyosin. Chains of grey balls are actin, red balls are troponin and blue dots are myosin binding sites (Modified from Lehman, Craig, & Vibert, 1994).

2.2 Force-velocity relationship

The force-velocity relationship is an important feature of muscle contraction. It establishes that the relationship between load and velocity of shortening generated by the muscle is inversely proportional (Fenn & Marsh, 1935). The force-velocity relationship was first characterized as a polygonal hyperbola, based on Hill's groundbreaking studies with frog muscles (Hill, 1938). This hyperbola can be explained by the following equation:

$$(P+a)\,(V+b) = (P_0+a)\,b$$

where, P is force, a represents the constant shortening unit with the dimension of the load, imposed to the system, V is velocity, b expresses the constant increase energy rate per unit of decrease in load with the dimension of velocity, and P_o is the isometric force. Subsequent studies have shown a small deviation from the rectangular hyperbola (Figure 7) at high isometric forces (Bahler, Fales, & Zierler, 1968; Edman, 1979; Edman & Hwang, 1977; Edman, Reggiani, & te Kronnie, 1985). This biphasic shape of the force-velocity relationship (Figure 7) fits the following equation (Edman, 1988; Rassier, 2010):

$$v = \frac{(P_0^* - P)b}{P + a}\,(1 - \frac{1}{1 + e^{k_1(p - k_2 P_0)}})$$

The first term of the equation expresses the force-velocity relationship if the force is less than 0.78 P_0 and P_{0*} ratio is the isometric force predicted from the rectangular hyperbola. The second term is the correction term of the Hills equation if the force is greater than 0.78 P_0 with k_1 and k_2 as constants.

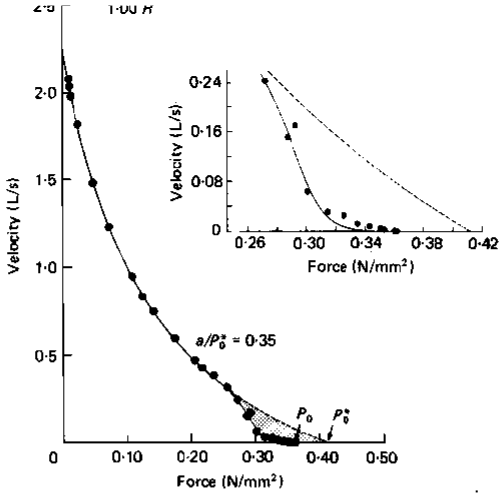

Figure 7. A double hyperbolic force-velocity relationship derived from experiments with single muscle fibers. The continuous line fit with the double hyperbolic force-velocity equation and the dashed line extrapolates the hyperbola derived from the force lower than 0.78 P_0. Inset: the details of high force-velocity relationship shown in the main diagram (Adapted from Edman, 1988).

2.3 In-Vitro Motility Assay (IVMA) to investigate the myosin-driven sliding of actin filament

The IVMA was developed to study the actin-myosin interactions and velocity of actin sliding, by investigating the motility of actin over myosin filaments (Kron & Spudich, 1986). In this assay, the sliding velocities of florescent labeled actin on a myosin coated microscope

coverslip is measured in the presence of ATP. This sliding velocity produced by the myosin ultimately corresponds to the shortening velocities of muscle (Howard, 2001). The maximum shortening velocity (V_{max}) depends on both the displacement (d) produced by the single myosin filament and the period of time myosin strongly bound with actin (t_{on}). As such, the actin filament velocity or maximum shortening velocity, is represented with the following equation (Tang et al., 2016; Warshaw, 2004):

$$V_{max} = d / t_{on}$$

2.4 Fiber type characteristics

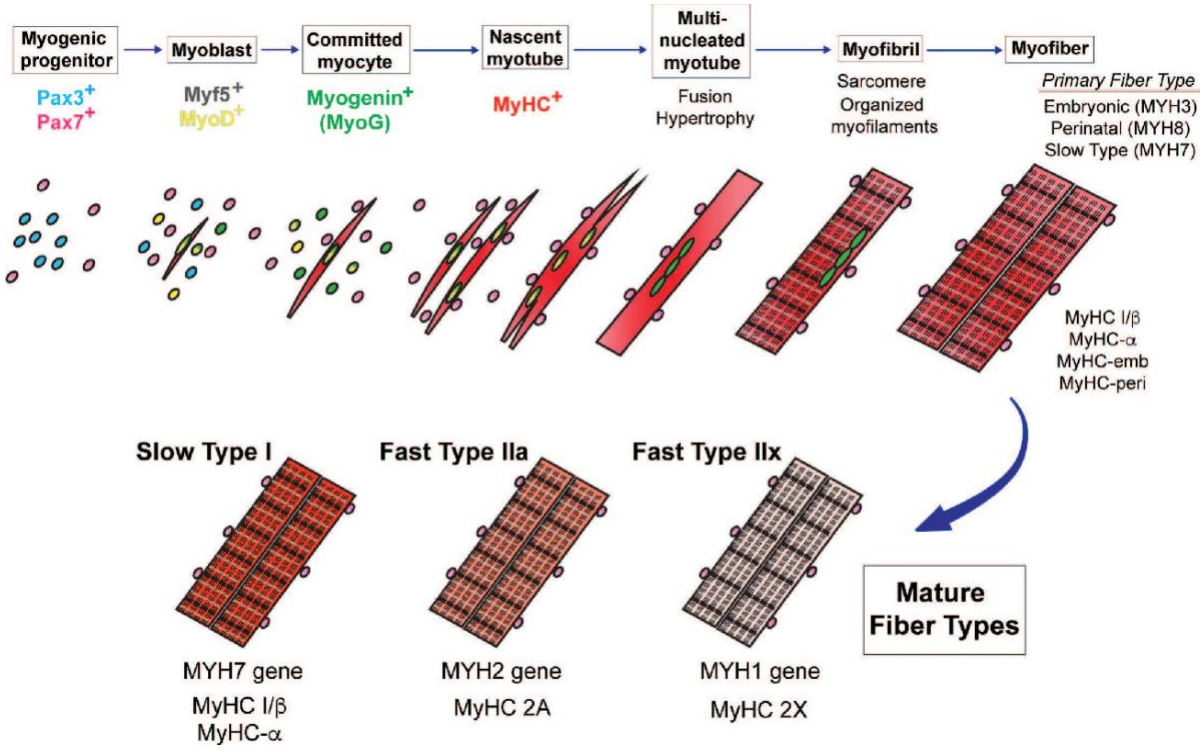

Figure 8. The differentiation and fiber type specification of skeletal muscles. Actin, myosin and elastic myofilaments are arranged in parallel within sarcomeres, which are in turn arranged concentrically within the myofibril. Different isoforms define three mature fiber types: slow type I, fast type IIA and fast IIX (Adapted from Glaser & Suzuki, 2018).

The functional flexibility of a muscle fiber type and the motor unit size allow a muscle to perform different tasks according to specific demands (Bottinelli & Reggiani, 2000). The diversity among skeletal muscle fibers enhances muscle activity and performance. A specific profile of gene expression is responsible for muscle fiber type determination and functional properties. These genetic profiles determine the MyHC isoform composition (Figure 8). MyHC isoform is the most commonly used method for classifying muscle fiber types (Polla, D'Antona, Bottinelli, & Reggiani, 2004). According to immunohistochemical analysis, human skeletal muscle consists of three fiber types (Table 1) characterized by their MyHC isoforms (Arbanas et al., 2009; Staron, 1997). Skeletal muscle fibers can also be classified based on structural or functional characteristics (Table 1). However, these structural and functional characteristics can be changed depending on physiological states (e.g. extreme training and age) or pathological conditions (e.g. respiratory and cardiovascular diseases) (Polla et al., 2004).

Fiber type classification:			
Myosin based	Slow or type I	Fast or type IIA	Fast or type IIX
Based on metabolism & time	Slow oxidative (SO)	Fast oxidative (FOG)	Fast glycolytic (FG)
Based on fatigue resistance	Slow fatigue resistance (S)	Fast fatigue resistance (FFR)	Fast fatigable (FF)
Properties:			
Maximum shortening velocity	Slow	Fast	Very fast
Myofibrillar ATPase activity	Low	High	Very high
Time course of the twitch	Slow	Fast	Fast

Table 1. Classification of skeletal muscle fiber based on myosin types, metabolism, time and fatigue resistance along with distinctive molecular properties of each fibers (Adapted from Polla et al., 2004).

2.4.1 Diaphragm

The word diaphragm is derived from the Greek words *dia* (in between) and *phragma* (fence). Characterized by small fiber size, high aerobic oxidative enzymatic activity and large quantities of capillaries, the diaphragm is highly resistant to fatigue. It is a musculofibrous dome-shaped structure located in between the thoracic and abdominal cavity (Maish, 2010) (Figure 9). The diaphragm allows for voluntary and involuntary control of respiration via continuous contraction and relaxation, while extra diaphragmatic muscle (accessory respiratory muscle) only contribute to increasing ventilation depth (Polla et al., 2004). The diaphragm also has non-respiratory functions, which include separating thoracic and abdominal cavities, increasing intra-abdominal pressure and exerting control over the lower esophageal sphincter (Kolar et al., 2009; Maish, 2010). There is considerable evidence suggesting that the adult human diaphragm is composed of about 55% slow or type I fibers, 21% fast oxidative or type IIA fibers, and 24% fast glycolytic or type IIX fibers (Lieberman, Faulkner, Craig, & Maxwell, 1973; Mizuno, 1991; Sanchez, Medrano, Debesse, Riquet, & Derenne, 1985). Small laboratory animals (rats and mice) have a higher proportion of fast fibers in respiratory muscles as well as more aerobic oxidative activity compared to humans or large animals like rabbits (Blank, Chen, & Ianuzzo, 1988; Hodge et al., 1997; Polla et al., 2004).

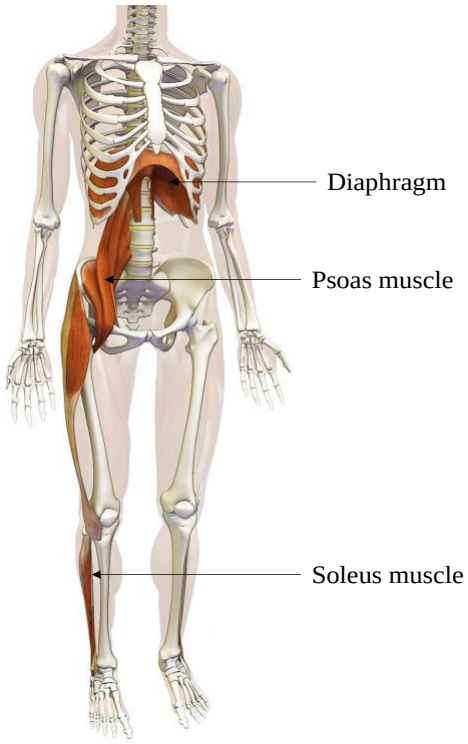

Figure 9. The diaphragm is the dome-shaped muscle that separates the chest and abdominal cavities. It originates at the sternum and is inserted into the central tendon. The psoas muscle connects the lumbar vertebra to the femur. It mostly helps to flex the hip joint and aids in lifting the upper leg towards the body. The soleus muscle is the powerful muscle helps planter function of foot located at the distal region of the leg, extending from the knee to the heel.

2.4.2 Soleus and psoas muscle

The human soleus is a flat, calf muscle located beneath the gastrocnemius muscle (Bolsterlee et al., 2018; Gollnick, Sjodin, Karlsson, Jansson, & Saltin, 1974) (Figure 9). It joins with the gastrocnemius to attach to the Achilles tendon. It produces force and mechanical work during human walking and running by plantarflexion and it also plays a vital role in controlling balance (Lai et al., 2015). This muscle contains predominantly slow or type I muscle fibers (80%)

which are highly resistant to fatigue, specializing it for aerobics and endurance-type activities. However, it has reduced ability to produce powerful movements for prolonged time due to a small percentage (20%) of type II or fast muscle fibers (Gollnick et al., 1974).

The psoas major is a long fusiform skeletal muscle which connects the vertebral column to the lower limb and aids in dynamic and postural functions (Siccardi & Valle, 2018). This active postural muscle is responsible for the hip flexion, lateral rotation and adduction of the hip joint (Figure 9). It consists of 60% fast or type II fibers and of 40% slow-twitch or type I fibers. It is therefore very distinct from the diaphragm muscle (Arbanas et al., 2009).

3. Hypertrophic Cardiomyopathy (HCM)

Cardiomyopathies are defined by structural and functional abnormalities of the cardiac myocyte and are associated with dysfunction of the heart and other organs. The World Health Organization (WHO) classifies a wide range of cardiomyopathies into the following groups: hypertrophic cardiomyopathies, dilated cardiomyopathies, restrictive cardiomyopathies and arrhythmogenic right ventricular cardiomyopathies (Harvey & Leinwand, 2011). HCM, also known as hypertrophic obstructive cardiomyopathy and idiopathic subaortic stenosis, is one of the most common inherited cardiac diseases, affecting 1 in every 500 people (Maron, 2002). Epidemiological studies suggest that cardiomyopathies are caused by a wide spectrum of mutations and clinical manifestations. As a result, there is a wide array of prognoses and treatment protocols. It is the leading cause of sudden cardiac death in young individuals and competitive athletes (Fatkin & Graham, 2002).

3.1 Clinical presentations

In general, HCM leads to unexplained left ventricular hypertrophy (LVH) (Figure 10) in a preexisting non-dilated ventricle in the absence of other cardiac diseases, such as systemic hypertension or aortic stenosis. Clinical manifestations of HCM from early childhood to late adulthood are broad and highly variable ranging from an asymptomatic murmur and life-threatening heart failure to sudden cardiac death. An individual with HCM typically exhibits the following symptoms: shortness of breath during exertion, chest pain, fainting, palpitations, orthostasis and syncope (Cirino & Ho, 1993; Ho et al., 2018). Comorbidities include generalized muscle weakness, decreased inspiratory muscle strength and decreased maximal inspiratory pressure, which is associated with alteration of respiratory and distal skeletal muscle strength (Hammond, Bauer, Sharp, & Rocha, 1990; Lecarpentier, Coirault, Langeron, et al., 1999).

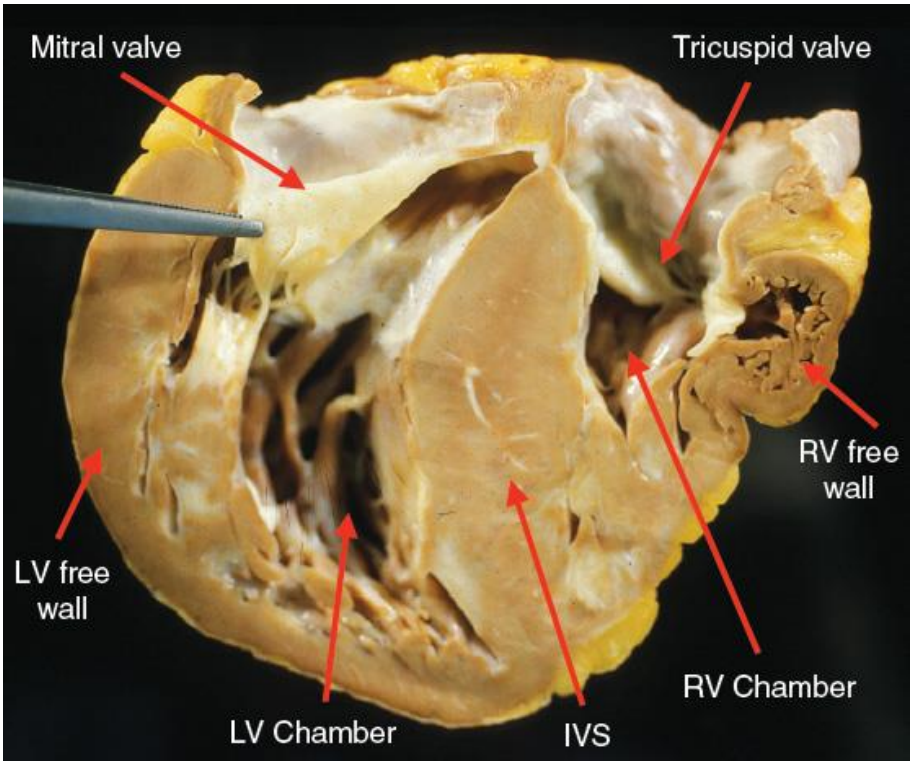

Figure 10. Pathologic specimen of the human heart with HCM demonstrating asymmetric septal hypertrophy causing left ventricular (LV) outflow obstruction. The patchy fibrosis and small thick-walled arterioles are grossly demonstrated predominantly in the interventricular septum (Adapted from Kasper, 2015).

It is important to diagnose the HCM as early as possible in order to prevent fatal outcomes, especially in young patients. Early diagnosis of cardiomyopathies is possible by using echocardiography to evaluate for an increased ventricular wall thickness, decreased left ventricular chamber size and compromised systolic function (Figure 10). HCM characteristics are more evident in elderly patients, while few morphological differences, like septal curvature and malformation of left ventricular outflow, can be seen in younger patients (Lever, Karam, Currie, & Healy, 1989; Lewis & Maron, 1989; Wigle, Rakowski, Kimball, & Williams, 1995). Macroscopically, asymmetric septal hypertrophy is the most common pattern of hypertrophy (figure 10). Hypertrophy could be confined to a wall or in the apex of the left ventricle which can be established by non-invasive cardiac imaging like echocardiography and cardiac magnetic resonance imaging (Maron, 2002; Nishimura, Ommen, & Tajik, 2003).

3.2 Histologic abnormalities

In HCM, cardiac dysfunction initially exhibits a change in cellular morphology and an increased cardiac mass. Specifically, an asymmetrical interventricular septal thickening can be observed in HCM. Histopathological hallmarks include myocyte hypertrophy, myofibrillar disarray, perivascular and interstitial fibrosis (figure 11) (Ho & Seidman, 2006). This ventricular myocyte hypertrophy develops in response to altered contractility in order to keep heart adaptation

to higher functional demands. Myofibrillar disarray is mainly distributed on the left ventricle wall and it is more commonly seen in young patients (Fatkin & Graham, 2002). Interstitial perivascular fibrosis composed of collagen types 1 and 3 interrupts the coupling between cardiomyocytes and increases myocardium stiffness, which ultimately lowers the contractile capacity of the heart. Normal coronary circulation is interrupted by thickened arteries with higher collagen and narrow lumen wall, eventually causing myocardial ischemia. This continuous cardiac architectural alteration in HCM decreases the cardiac output, which in turn can lead to heart failure (Harvey & Leinwand, 2011).

A **B**

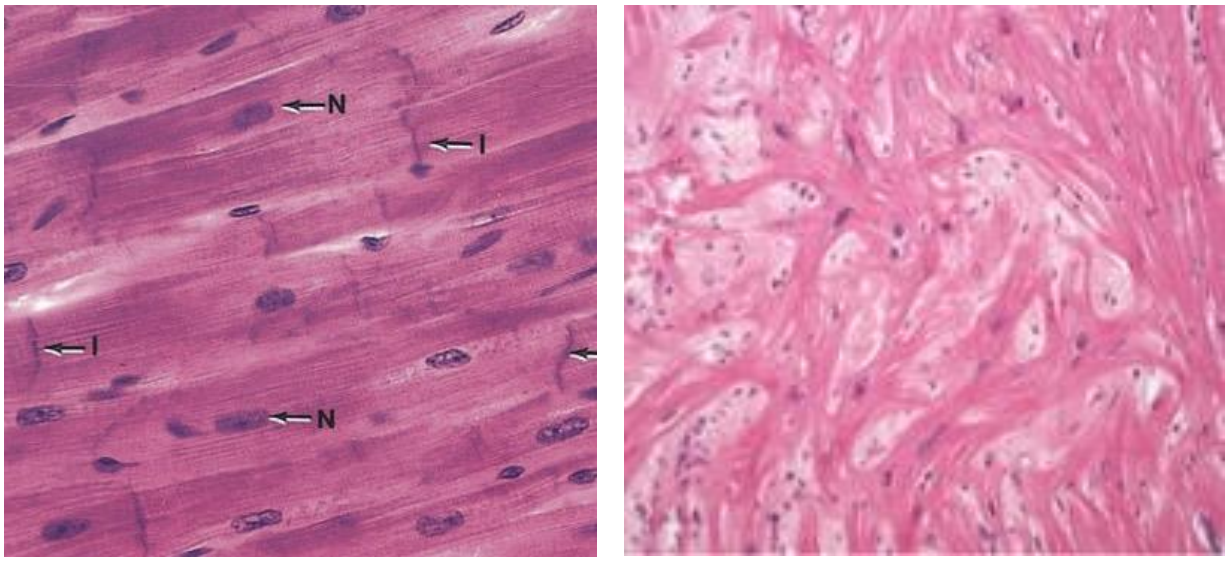

Figure 11. (A) Microscopic picture of a normal cardiac muscle demonstrating intercalated disks (I) which cross the fiber and nuclei (N) at the center of the muscle fibers. (Adapted from Mescher & Junqueira, 2016) (B) Microscopy of a cardiac muscle in HCM condition indicating characteristics features such as misaligned and disarrayed myocyte fibers, myocyte hypertrophy and interstitial fibrosis (Adapted from Kasper, 2015).

3.3 Genetic involvement

Mutations causing HCM have an autosomal dominant inheritance, with consequences in several sarcomere proteins. HCM affects approximately 50-60% of probands with a positive family history (Cirino & Ho, 1993; Harvey & Leinwand, 2011). More than 400 different mutations in 13 sarcomeric proteins have been identified in association with HCM. Among them, mutations in the cardiac β-MyHC, components of thick filaments, were the first to be identified and responsible for ~35-50% of all cases. The MYH7 gene plays a vital role in β-MyHC transcription, which is commonly found in the cardiac and slow skeletal muscle. The β-MyHC forms a greater portion of the myosin type II protein which produces mechanical force during muscle contraction (Tajsharghi & Fyhr, 2008). It has been suggested that the amino acid residues encoded by the MYH7 gene are critical for myosin function due to their high conservation throughout evolution (Lamont et al., 2014). The mutation in the cardiac β-MyHC not only affects the contractile proteins but also numerous other proteins, like the essential and regulatory myosin light chain, myosin-binding proteins C, α-MyHC, titin, as well as the components of thin filaments such as cardiac troponin T, troponin I and α-tropomyosin (Elliott et al., 2014; Fatkin & Graham, 2002). The severity and onset of symptom depend on the type and location of HCM-causing genes. For example, β-MyHC mutations usually appear during the first two decades of life while MyBP-C mutations are typically asymptomatic until the fifth or sixth decades of life (Niimura et al., 1998).

3.3.1 R403Q mutation

The mammalian heart has two types of cardiac myosin isoforms; α-MyHC and β-MyHC isoforms. Among them, α-MyHC is found mostly in the atria, while β-MyHC is expressed predominantly in the ventricles and slow skeletal muscle fibers (Malmqvist, Aronshtam, & Lowey,

2004). β-MyHC is the major protein of the myosin thick filament, which is involved in heart muscle contraction as well as slow skeletal (type I) muscles. Among the 13 genes encoding sarcomeric proteins which are associated with HCM, β-MyHC has been identified in 35-50% of cases (Marian et al., 1999). Both myosin isoforms are 93% identical in amino acid sequence but exhibit significantly different enzymatic properties due to non-identical residues in functional domains (Lowey et al., 2018). For example, the α-MyHC isoform has a 2-fold greater unloaded shorting velocity but a 2-fold lower isometric force when compared to β-MyHC isoform (Malmqvist et al., 2004). The absolute values of myosin ATPase activity and actin activated sliding velocities depend also on the species used for myosin purification; small mammals show higher ATPase rates compared to large ones (Malmqvist et al., 2004).

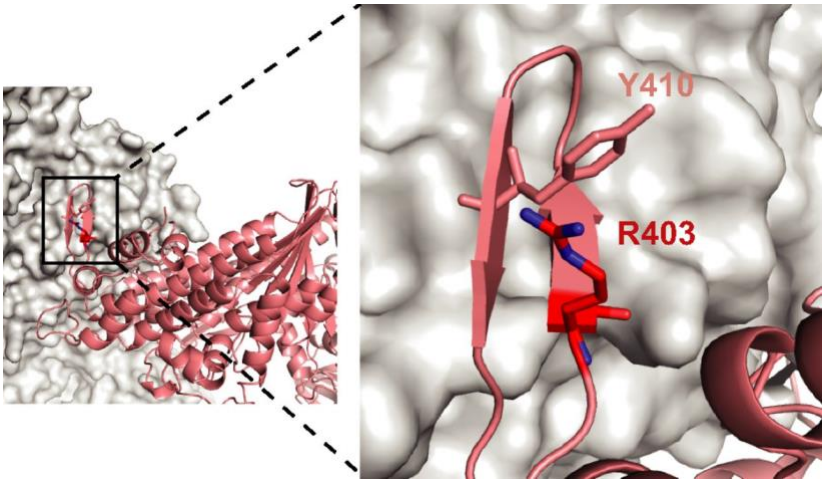

Figure 12. Crystal structure of the cardiomyopathy loop (CM-loop) at the actin-myosin interface. An antiparallel β-strand is formed by the CM-loop which is a key site of interaction with actin (gray color). This organized loop is preserved in all myosin II isoforms and stabilized by interacting with actin. The R403Q mutation in β-cardiac myosin cause the arginine (R) 403 (red color) interaction with a tyrosine residue on the neighboring β-strand on the actin CM-loop with actin become weak due to the presence of a mutation at this site (Adapted from Lowey et al., 2018).

Approximately 300 mutations have been identified in the β-MyHC, leading to a wide spectrum of cardiac diseases, which vary in severity (Lowey et al., 2018). The cardiomyopathy loop forms an antiparallel β strand conserved in all myosin II isoforms and is stabilized when interacting with actin. R403Q is a point mutation in exon 13 of the β-cardiac MyHC gene where an arginine residue (Arg-403) is converted to a glutamine on a neighboring β strand (Figure 12). This mutation of β-cardiac myosin ultimately disrupts the interaction of the cardiomyopathy loop with actin and decreases the functional activity of myosin (Geisterfer-Lowrance et al., 1990; Lowey et al., 2018). It is the first and most extensively studied missense mutation responsible for familial HCM, an autosomal dominant heterogeneous cardiac disease (Cirino & Ho, 1993). The high incidence rate of sudden cardiac death and high penetrance rate makes the R403Q mutation unique. The cardiomyopathic phenotype is expressed in more than 90% of individuals with a positive genotype at an early age, and more than 50% of individuals end up with sudden cardiac death (Ferreira et al., 2010). There is controversy about the myosin domain location of cardiomyopathies and skeletal myopathies due to various phenotypes of MYH7 gene. Thus, it is difficult to explain the phenotypic variance of MYH7 gene related myopathy with the monogenic mutation sequences (Ko, Lee, Jang, Jang, & Ryu, 2019).

3.3.2 Animal model

The origin of the genetic disease starts with the development of gene dysfunction. A rabbit model of HCM has been generated by injecting purified transgenes into fertilized zygotes. Northern blotting and gel electrophoresis have been performed to confirm the expression of transgene mRNA (Marian et al., 1999). There is also a mice model that was developed by injecting embryonic stem cells containing missense mutations on one allele into the mouse blastocysts to

get chimeras of homozygous and heterozygous mice (Geisterfer-Lowrance et al., 1996). There are a few common phenotypic characteristics observed in both the transgenic, TG+ rabbit and mice models. Premature death, histopathological abnormalities, cardiac dysfunction like myocyte and myofibrillar disarray, interstitial fibrosis, systolic and diastolic abnormalities can be seen in both models (Geisterfer-Lowrance et al., 1996; Marian et al., 1999). However, left ventricular hypertrophy is the key feature of human HCM patients which is present in the TG+ rabbit model but minimal in the mice model. The left ventricular systolic function is impaired globally in TG+ mice while it is affected regionally in humans and rabbits (Marian et al., 1999). MyHC isoforms can alter the phenotypic response of the heart by affecting the speed of muscle shortening and cross-bridge kinetics (Lowey et al., 2018). It has been shown that β-MyHC mutation is responsible for human HCM which is similar to the rabbit model.

3.4 Skeletal muscle performance in HCM

Patients with HCM suffer from angina, breathlessness, arrhythmia and sudden death. Sudden cardiac death due to heart failure typically takes place after vigorous activity with a mortality rate of 2-3% for adults and 4-6% for young adolescents (Ralston, Penman, Strachan, & Hobson, 2018). These effort-related symptoms, especially breathlessness, occurs due to an increase in the airflow resistance and a decrease in the compliance of the respiratory systems (Gehlbach & Geppert, 2004). There are alterations in the respiratory muscle perfusion and an increased ventilator load, indicating respiratory muscle weakness (Lecarpentier, Coirault, Langeron, et al., 1999; Mancini, Ferraro, Nazzaro, Chance, & Wilson, 1991). Peripheral muscle weaknesses during heart failure has also been reported, but the frequency and severity are much

higher in inspiratory muscles (De Sousa et al., 2001; Lindsay et al., 1996). The reduction of lung volume and diffusion capacity has been observed in cardiomyopathy patients with chronic heart failure (Witt et al., 1997).

The diaphragm also undergoes molecular adaptations as a result of HCM, such as muscle fiber type shifting, muscle atrophy and alteration in intracellular calcium regulation (Gillis et al., 2016; Lecarpentier, Coirault, Riou, Chemla, & Mercadier, 1999; MacFarlane, Darnley, & Smith, 2000; Supinski, DiMarco, & Dibner-Dunlap, 1994). The fiber shift from fast fatigable to slow oxidative fiber happens due to endurance adaptation, as the diaphragm needs to keep up with a high workload. These changes occur both in diastolic and systolic dysfunction (Lavietes, Gerula, Fless, Cherniack, & Arora, 2004; Meyer et al., 2001; J. P. Ribeiro, Chiappa, Neder, & Frankenstein, 2009).

In a study with the rabbit diaphragm after congestive heart failure, a reduction in the force production by myosin cross-bridges as well as a decrease in the total number of cross-bridges attached to actin in a given time during contraction was observed (Lecarpentier et al., 1998). Another study with the rat diaphragm suggested a shift in the muscle fiber type, making the muscle more fatigable (Stassijns et al., 1999). Additionally, reduction in maximal force generation, rate of force redevelopment and calcium sensitivity was observed in single muscle fibers isolated from diaphragm in mice with HCM causing CHF (van Hees et al., 2008; van Hees et al., 2007).

It has been established that the mutation of the β-MyHC gene responsible for HCM is also present in skeletal muscle. The slow skeletal muscle soleus with HCM mutation demonstrates abnormalities in the velocity of actin sliding contraction. It also shows central core disease (CCD) (Fananapazir et al., 1993), a rare autosomal dominant myopathy with the predominant in type I fiber in the absence of mitochondria.

4. Summary

It has been shown that respiratory muscle performance is lower in patients with HCM. It has also been shown that the HCM mutation in the heart are associated with skeletal myopathy. However, the mechanism behind such myopathy and reduced contractile function has not yet been determined. The asymptomatic development of HCM, difficult phenotype prediction and limited access to patient's diaphragm samples make it difficult to understand the mechanism of respiratory weakness in this disease.

Rationale

The following study aimed to assess the respiratory and skeletal muscle alterations in a rabbit model with HCM. We selected skeletal muscles with different type of fiber composition. The diaphragm, chief respiratory muscle composed of both slow and fast fibers; the soleus, a powerful lower limb muscle contained predominantly slow twitch fibers and the psoas, a deep-seated core muscle composed mostly of fast fibers. We evaluated the contractile properties of the diaphragm, soleus and psoas muscle of rabbits with a R403Q mutation in the heart.

The main objective of this study was to investigate whether there was a loss of contractile function at the molecular level in the diaphragm, slow and fast skeletal muscles association with mutation in β-MyHC of the heart. Our hypothesis was that the diaphragm and the soleus muscles from rabbits containing the heart mutation (TG+) would present a loss of contractile function.

CHAPTER 2 - EXPERIMENTAL ARTICLE

Contractile properties of skeletal muscles in hypertrophic cardiomyopathy

Md Rezuanul Haque Saikat[1], Dilson E. Rassier[1]

[1]Department of Kinesiology and Physical Education, McGill University,

475 Pine Avenue West, Room 308

Montreal, Canada

October, 2019

Abstract

Background: HCM is a deadly cardiovascular disease caused by mutations in the cardiac muscle proteins. There is evidence that the diaphragm and other skeletal muscles are weakened in patients with HCM. However, the mechanism behind this muscle dysfunction yet to be revealed at the molecular level. In this study, we investigated the functional performance of skeletal diaphragm, soleus and psoas muscle in a rabbit model of HCM with a R403Q mutation in the β-MyHC. We hypothesized that the contractile protein of diaphragm and soleus muscle taken from transgenic (TG+) rabbit from R403Q mutation will produce less velocity of actin sliding over myosin and ATPase activity compared to the sample taken from wild type (WT) animals.

Methods: Two different types of experiments (in-vitro motility assay and actin activated ATPase activity) were performed on purified myosin and heavy meromyosin (HMM) of the diaphragm, soleus, and psoas muscles of WT and TG+ rabbits to assess the sliding velocity and ATPase activity.

Results: The TG+ HMM samples from diaphragm and soleus muscles produced 16% and 22% lower actin sliding velocity than WT HMM, respectively. The ATPase activity of TG+ diaphragm and soleus myosin and HMM were also lower than WT samples. However, there was no difference in the velocity and ATPase activity for the psoas muscles between the two groups.

Conclusion: Mutation in the heart that causes HCM can alter the contractility of the diaphragm and soleus muscles, hence causing a loss of function.

Introduction

HCM is the most common form of inherited cardiomyopathy (1:500 in the general population) characterized by thickening of the cardiac wall, contractile dysfunction and arrhythmias (Maron, 2002; Nishimura et al., 2003). It can be defined as a sarcomeric disease where distinct mutations of the cardiac β-MyHC gene (MYH7) detected on chromosome 14 affect the sarcomere contractile proteins (Tajsharghi & Fyhr, 2008). This autosomal dominant disease is identified as the primary cause of sudden cardiac death of young athletes under the age of 35 (Maron, 2002). Surprisingly, the rates of death and cardiac transplants associated with this disease reach up to 20% in infants (Colan et al., 2007). The clinical manifestation depends on which proteins in the cardiac sarcomeres are mutated, ranging from asymptomatic to end-stage of cardiac failure, or sudden death. The symptoms include dyspnea, chest pain, fainting, palpitations, orthostasis, and syncope (Cirino & Ho, 1993; Greaves, Roche, Neutze, Whitlock, & Veale, 1987; Ho, 2010; van der Velden & Stienen, 2019). Shortness of breath or dyspnea, especially during exertion, is associated with inspiratory muscle weakness, and decreases the maximal inspiratory pressure which ultimately impairs the exercise capacity (Hammond et al., 1990; Lecarpentier, Coirault, Langeron, et al., 1999; Meyer et al., 2001). This alteration of diaphragm muscle in condition of cardiomyopathy has been observed without any changes in ventilatory drive (Bales & Sorrentino, 1997; Witt et al., 1997). Cardiomyopathy has also been associated with impairing limb muscle performance (Darin, Tajsharghi, Ostman-Smith, Gilljam, & Oldfors, 2007).

The chief respiratory muscle, the diaphragm, presents functional and histological abnormalities in several clinical studies pertaining to cardiomyopathy and heart failure (Fatkin et al., 2000; Ho, 2010; Meyer et al., 2001; J. P. Ribeiro et al., 2009). The diaphragm undergoes atrophy, reduced contractile function and an increased workload due to sarcomere disruption in

congestive cardiac failure (Lieber, Schmitz, Mishra, & Friden, 1994; Zhu, Petrof, Gea, Comtois, & Grassino, 1997). A relative increase of slow oxidative fibers can also be seen in muscle biopsies taken from the diaphragm of patients with cardiomyopathy (Howell et al., 1995). Additionally, HCM mutations affecting ventricular architecture, which contributes to cardiac myocyte hypertrophy, myofibrillar disarray, perivascular and interstitial fibrosis (Ho & Seidman, 2006; Spudich, 2014). This type of myopathy can be developed in slow type I skeletal muscle like diaphragm and soleus, owing to homologous protein mutations in their sarcomeres (Cuda, Fananapazir, Epstein, & Sellers, 1997; Cuda et al., 1993; Palmiter et al., 2000). There is evidence that cardiomyopathy also causes myopathy in limb or distal skeletal muscles (Fiorillo et al., 2016; Jandreski, Sole, & Liew, 1987; Jasmin & Proschek, 1982). For instance, the soleus muscle manifests functional and structural disruption in the presence of the HCM mutation (Fananapazir et al., 1993). Finally, there is indirect evidence suggesting that the number of myosin cross-bridges interacting with actin and the force produced by the myosin molecules decreases, ultimately impairing muscle relaxation of the diaphragm (Lecarpentier et al., 1998).

Despite the fact that cardiac β-MyHC (MYH7) is expressed in both cardiac and slow type I skeletal muscle fibers, there are not many studies that have investigated skeletal muscles of HCM patients in the presence of a missense mutation in the MYH7 gene. As a result, the molecular mechanism responsible for lowering muscle performance has yet to be revealed (Cuda et al., 1997; Fananapazir et al., 1993).

The present investigation examines the relationship between HCM and skeletal muscles, with particular attention to the diaphragm as it can cause respiratory weakness. We also wanted to investigate the effect of HCM on psoas muscle composed predominantly of fast fiber type to compare with the diaphragm and soleus muscles. We used a rabbit model with an arginine to

glutamine point mutation at amino acid 403 (R403Q) in the MyHC gene, which encodes the β-MyHC. This was identified as the first missense mutation responsible for HCM (Geisterfer-Lowrance et al., 1990). This asymptomatic TG+ rabbit model is preferred to mice due to the size of the heart, echocardiography feasibility and the myocardial background that ~98% homologous to the human β-MyHC and exhibits complete phenotypic expression comparable to human HCM (Lowey et al., 2018; Marian et al., 1999). We examined the contractile performance of diaphragm, soleus and psoas muscles at the molecular level. Our results show that myosin of diaphragm and soleus muscles isolated from TG+ rabbits induce a decreased actin sliding velocities and ATPase activity in these muscles.

Methods

Protein purification

Individual skeletal muscles were carefully dissected from adult WT and TG+ New Zealand white rabbits and chemically permeabilized using standard procedures used in our laboratory (Campbell & Moss, 2002; Minozzo & Rassier, 2010). Muscles were incubated in rigor solution (50mM Tris, 100mM KCl, 2mM $MgCl_2$ and 1mM EGTA at pH 7.0) for 4 hrs and then transferred to a rigor-glycerol (50:50) (v/v) solution for 24 hrs. Then, the muscles were incubated in a new rigor solution mixed with glycerol and protease inhibitors (Sigma-Aldrich, Canada), and stored in a -20°C freezer. Animal use was approved by the McGill University Animal Care Committee and complied with the guidelines of the Canadian Council on Animal Care.

Myosin was isolated from the psoas, soleus, and diaphragm of WT or TG+ rabbits using a protocol that has been previously described (Cheng, Matusovskiy, & Rassier, 2018; Fonseca, Cachaldora, & Carballo, 2013; Kalganov et al., 2013; Yutaka et al., 2010), with minor

modifications. The biochemical and molecular mechanics measurements were performed within 24 hrs of purification to ensure the functionality and freshness of myosin (Homsher, Wang, & Sellers, 1992). On the day of myosin purification, 5g of muscles were weighed and minced before being transferred to a fresh rigor solution and stored in the fridge for 2 hrs. The preparations were washed to remove soluble proteins. The washed residue was blended in an Omni mixer homogenizer (Omni International, Inc., Georgia, USA) with a Hasselbalch-Schneider buffer (0.1 M KH_2PO_4/K_2HPO_4 at pH 6.4; 0.6 M KCl, 10 mM $Na_4P_2O_7$, 1 mM $MgCl_2$, and 20 mM ethylene glycol tetraacetic acid (EGTA)). After homogenizing, the mixture was stirred continuously for 15 min at 4°C. The extraction was stopped by the addition of 20 mL of 4°C distilled water. The insoluble residues were removed from the extract by centrifugation at 3,000×g for 10 min in cold, while the supernatant (myosin solution) was filtrated through a filter paper (No. 54, GE healthcare companies, UK). The filtrate was diluted with two-fold distilled water at 4°C and centrifuged at 10,000×g for 15 mins to get myosin precipitation. The myosin pellet was washed with buffer (20 mM K_2HPO_4 at pH 7.2; 0.12 M KCl; 1 mM Ethylene diamine tetraacetic acid (EDTA) and 1 mM DL-Dithiothreitol (DTT)) and centrifuged at 20,000×g for 10 min. The supernatant was discarded, and the pellet was washed with buffer D (50 mM Sodium Pyrophosphate and 1 mM DTT) and centrifuged again at 10,000×g for additional 15 min. Finally, the supernatant was filtered (No. 54 filter paper, WHATMAN™, GE, USA) to get the myosin solution. The myosin solution always kept and stored at 4°C during the entirety period of the experiment.

Purified myosin was used as an initial source for HMM purification using the previously described method (Cheng et al., 2018; Kron, Uyeda, Warrick, & Spudich, 1991). Briefly, the myosin stock solution was diluted nine times with BED solution (0.1 mM $NaHCO_3$, 0.1 mM EGTA, and 1 mM DTT) and mixed gently. After a period of 15 mins on ice, the solution was

centrifuged at 25,000×g for 10 min to sediment myosin filaments. The pellet was dissolved in an equal volume of 2×CHB solution (20 mM imidazole-HCl, 1 M KCl, 4 mM $MgCl_2$, and 10 mM DTT, pH 7.4). The myosin solution was incubated for 10 minutes at 25°C in the water bath (2239-Isotemp®, Fisher Science, USA). α-chymotrypsin (C-3142; Sigma-Aldrich, Canada) was added to the myosin solution to reach a final concentration of 12.5 μg/ml. After 10 min of proteolysis, the reaction was stopped by adding nine volumes of BED solution, with additional 3 mM $MgCl_2$ and 0.1 mM PMSF. The solution was kept on ice for 1 hour. The suspension was clarified by centrifugation at 25,000 g for 90 min. The supernatant containing HMM was collected, concentrated and stored at 4°C freeze before the experiments.

For polymerization of G-actin (AKL99, Cytoskeleton, Inc. USA) into a filamentous form (F-actin), a storage buffer (25mM Imidazole, 0.25mM $CaCl_2$, 0.2mM ATP and 0.5mM DTT at pH 7.4) was mixed with the G-actin and kept on ice for 1 hour. Then the solution was mixed with actin polymerization buffer (500mM KCl, 20mM $MgCl_2$, and 10mM ATP) and stored at a 4°C. The actin filaments were labeled for fluorescence with Alexa-488-phalloidin fluorescence dye (absorption/emission peaks at 488–520 nm) for visualization under fluorescence microscopy during IVMA. The concentrations of myosin and HMM were measured colorimetrically at a 595nm wavelength with a commercial Quick Start Bradford Protein Assay (Bio-Rad Laboratories, CA, USA) in triplicate.

In-vitro motility assays (IVMA)

The velocity and percentage of actin filaments sliding over myosin was measured with an IVMA following a protocol previously described in our laboratory (Cheng et al., 2018; Kalganov et al., 2013), with slight modifications. HMM was purified from muscles dissected from WT and

TG+ rabbits. A flow-through chamber was constructed using a glass microscope coverslip (22x50-1.5, Fisherbrand®, USA) coated with 1.0% nitrocellulose in amyl acetate (LADD Inc. VT, U.S.A). The temperature was maintained at 30°C throughout the experiments by using a system consisting of a water thermal exchange column (SC-20, Harvard apparatus, Canada). 100uL of 100µg/ml WT or TG+ HMM were passed through the chamber to allow it to randomly attach to the nitrocellulose that coated the coverslip for 1 min. 250 uL of assay buffer containing 0.1% fluorescence labeled actin filaments and 25 mM Imidazole, 25 mM KCl, 4 mM $MgCl_2$, 14 mM Glucose, 0.5 mM BSA, 0.018 mg/ml catalase, 0.1 mg/ml glucose oxidase, 17.8 mM dithiothreitol-containing 1 mM ATP and an oxygen-scavenging system was perfused in the flow-through chamber.

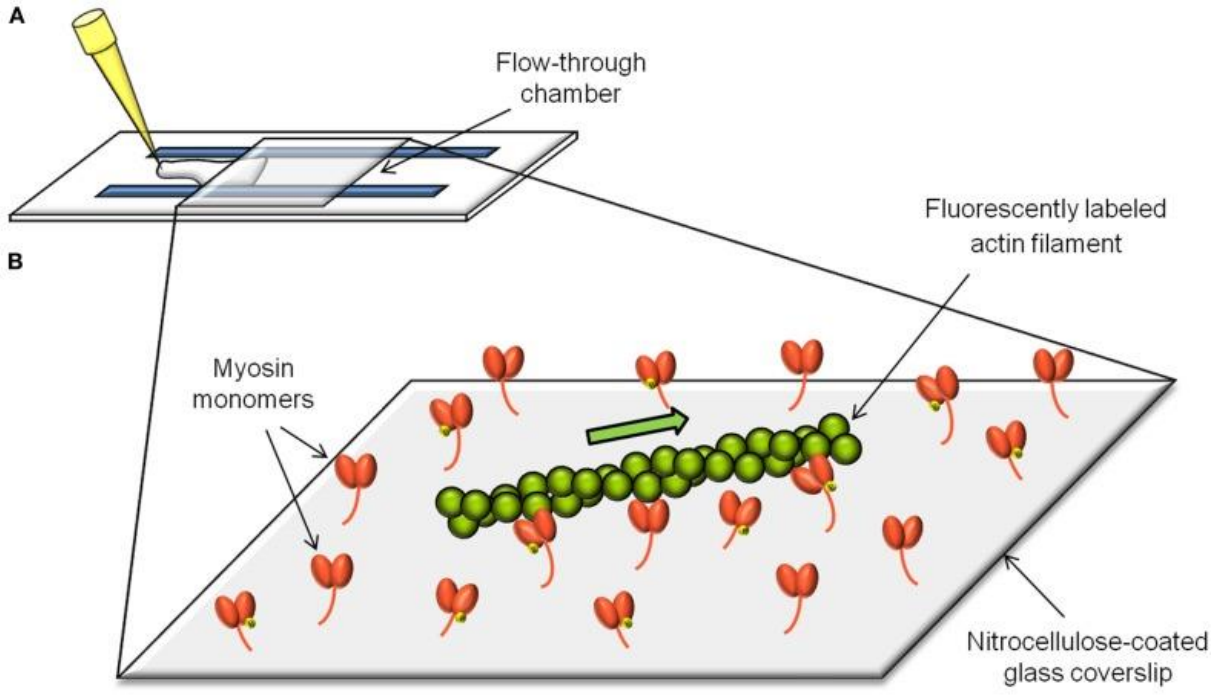

Figure 13. The schematic presentation of the IVMA. (A) The flow-through chamber of IVMA developed from a nitrocellulose-coated coverslip and a microscope slide. (B) The fluorescently labeled actin filaments set in motion randomly by myosin molecules observed under fluorescence microscopy (Adapted from Lauzon et al., 2012).

The velocities by which WT and TG+ HMM propelled the actin filaments were measured at different periods of times (3-15 minutes). The actin filaments were fluorescently imaged through a filter set using Exciter HQ480/40X, Dichroic Q505LP, Emitter HQ535/50 m, Chroma, USA; dye: Alexa-488. The fluorescent light signals emitted by the actin were collected with a 100X oil-immersion objective (Nikon, Plan Fluor, NA: 0.5–1.3). The video was recorded by a high-speed digital EMCCD Camera (Qimage, ROL-MGi-PLUS-F-M-14-C, 512 x 512 pixels BC, Canada). 150nm per pixels were analyzed in each video. Images of F-actin filaments were extracted from and tracked across video frames. The detection of actin sliding velocity was recorded and analyzed by a customized script written in Matlab software (MathWorks® 8.3.0, Massachusetts, U.S.A.) (Hilbert, Balassy, Zitouni, Mackey, & Lauzon, 2015; Hilbert et al., 2013). All the actin filaments were tracked and the motility velocity was calculated from the traces acquired from the complete tracking of an actin filament.

Actin-activated ATPase assays

The actin activated ATPase assays were performed in a temperature-controlled water bath at 25$_{o}$C. The Mg^{2+}-ATPase of myosin or HMM was calculated using a colorimetric assay through measurement of inorganic phosphate production (Matusovsky et al., 2015). The assay was performed in the presence of rabbit F-actin in a medium containing (in mM): 30 KCl, 0.1 $CaCl_2$, 0.5 $MgCl_2$, 2 DTT, 20 Imidazole-HCl (pH 7.2), following a modified Fiske and Subbarow method (Shelud'ko, Matusovsky, Permyakova, & Matusovskaya, 2007). The reaction was started after 10 min of incubation at 25°C by adding 1 mM of Mg^{2+}-ATP and was terminated after 10 min of incubation by adding 2.5% trichloroacetic acid. The ATPase activity expressed as of mole of

inorganic phosphate liberated for 1 min by 1mg of myosin or HMM was evaluated at 595nm wavelength by the equation:

$$ATPase\ activity = \frac{[Pi]}{Myosin\ concentration\ (mg)\ x\ time\ (min)}$$

Here, [Pi] can be calculated with coefficient from the calibrating curve [Pi] = 0.716 x OD595 x 2 (dilution factor) (Matusovsky, Mansson, Persson, Cheng, & Rassier, 2019).

Statistics

The data represent an average of multiple measurements from at least three myosin preparations. Comparison between groups were made using T-test. A significant level of $P<0.05$ was used for all comparisons. All values are presented as mean ± S.E.M.

Results

Actin sliding velocities

We examined the motility of actin driven by HMM using an IVMA. For the diaphragm and the soleus muscles, the sliding velocities produced by the HMM isolated from the TG+ muscles were significantly lower than that observed in HMM isolated from WT muscles (Figure 14).

We also measured the actin filament length (Figure 14) and motile fraction – the percentage of actin filaments that slide over the HMM in a given preparation (Table 2). There were no differences in actin filament length between the WT and the TG+ of these skeletal muscles during the IVMA. However, a significant decrease was observed in the motile fraction for the diaphragm

and soleus muscles of TG+ rabbit when compared to WT rabbit. The HMM isolated from psoas from WT or TG+ rabbits did not show any difference in the velocity of actin sliding or the motile fraction.

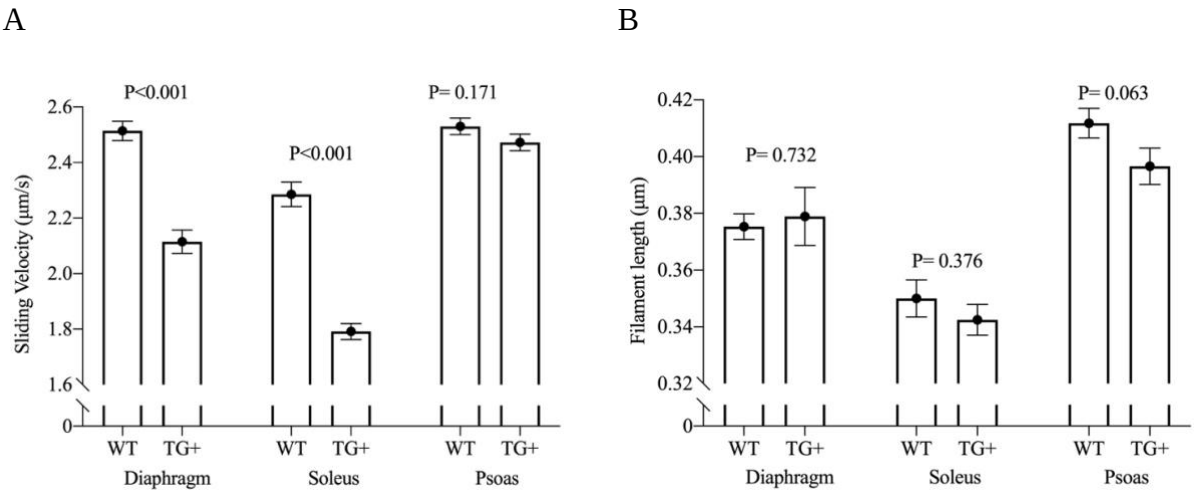

Figure 14. Actin filament velocities for the TG+ HMM compared with the WT rabbit HMM (A) The velocities are significantly different (P<0.001, t test) for the diaphragm (WT 2.514 ± 0.0352, n=384 and TG+ 2.115 ± 0.042, n=315) and the soleus (WT 2.285 ± 0.0439, n=309 and TG+ 1.792 ± 0.0286, n=417) HMM, but not for the psoas muscle HMM (P=0.171). (B) There were no changes in the actin filament length between WT and TG+ rabbit for diaphragm (P=0.732), soleus (P=0.376) and psoas (P=0.063).

Skeletal muscles	Motile fraction (%)	
	WT	TG+
1. Diaphragm	81.08	70.16
2. Soleus	82.10	73.31
3. Psoas	78.70	77.90

Table 2. Motile fraction of the experimental groups (WT and TG+).

Actin activated ATPase activity

To get further insight into the effects of cardiomyopathy on the skeletal muscle contractile proteins, we measured the ATPase activity of the actin-myosin complex from WT and TG+ rabbits (Figure 15). We found that the ATPase activity of TG+ myosin and HMM were significantly decreased in the diaphragm and soleus muscles compared to WT muscles. There was no significant difference in the ATPase activity in the psoas muscles from the TG+ fibers when compared to the WT fibers.

A B

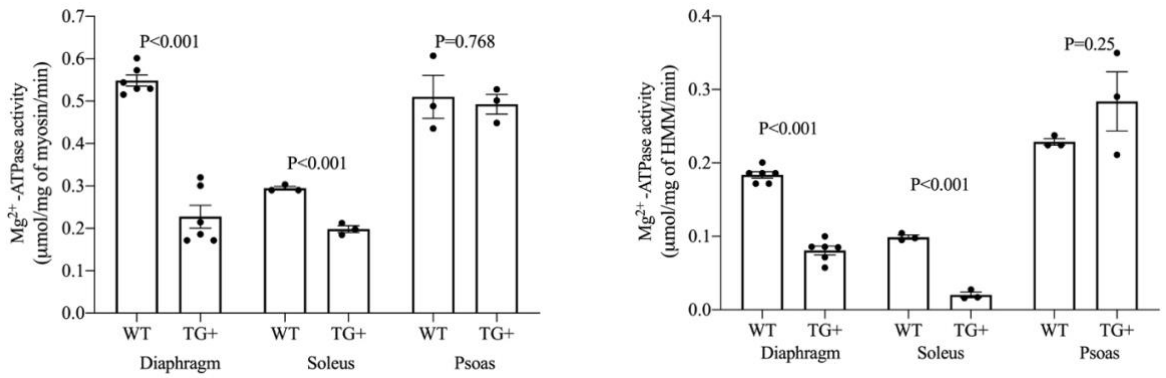

Figure 15. Actin-activated Mg^{2+}ATPase activity for WT and TG+ rabbit of diaphragm, soleus and psoas muscles. The data represent an average of multiple measurements from several myosin preparations. (A) The Mg^{2+}ATPase activity for the TG+ myosin of the diaphragm (TG+ 0.2276 ± 0.0271) and soleus (TG+ 0.1983 ± 0.0079) muscles were significantly lower compared to WT myosin diaphragm (WT 0.5489 ± 0.0132) and soleus (WT 0.2984 ± 0.0044) respectively. (B) The Mg^{2+}ATPase activity for the TG+ HMM of the diaphragm (TG+ 0.081 ± 0.0060) and soleus (TG+ 0.0203 ± 0.0037) muscles were also significantly lower compared to the WT HMM diaphragm (WT 0.1838 ± 0.0044) and soleus (WT 0.099 ± 0.0028) respectively, which follows the similar

pattern observed with the myosin preparations. Meanwhile, the psoas muscle does not show any differences when myosin was used (P=0.768) or HMM (P=0.245).

Discussion

The main finding of this study was a contractile function impairment at the molecular level of TG+ diaphragm and soleus muscles in condition of cardiomyopathy. Mutation in the cardiac β-MyHC gene reduced the actin sliding velocity and ATPase activity of diaphragm and soleus muscles, while no differences were found between TG+ and WT psoas muscles both in velocity and ATPase activity. There was also a decrease in the motile fraction for both diaphragm and soleus as a result of the mutation in the cardiac β-MyHC. A high percentage of the motile fraction of all muscles used in our experiments indicate the purity of HMM preparation.

This is the first study to evaluate the molecular contractile sliding of actin in both slow and fast skeletal muscles with the R403Q mutation in the heart. The developmental pathophysiology of a genetic disease varies depends on the pattern of inheritance, gene expression, environment, and lifestyle, among other factors (Ho et al., 2010). Additionally, different phenotypes have been associated with mutations of the same amino-acid residues in the β-MyHC (Ho, 2010). Therefore, the existence of mutations does not always lead to a recognizable disease due to the dissimilarity between genotype and clinical outcomes. It is challenging to explain the effect of HCM mutation on human skeletal muscle myosin function, given that small differences at the molecular level change many other parameters.

Our findings in slow skeletal muscle are consistent with results found in studies that performed with cardiac and skeletal muscles with the R403Q mutation in the β-cardiac myosin gene. A reduction in isometric force in a TG+ rabbit model with HCM mutation was observed in a study previously conducted in our laboratory (Lowey et al., 2018). In another study, soleus

muscle from HCM patients manifested in a decrease in isometric tension of type I fiber compare to healthy individuals (Malinchik, Cuda, Podolsky, & Horowits, 1997). Reduction in diaphragm contractility in a rabbit model with induced heart failure was observed in another study (Lecarpentier, Coirault, Langeron, et al., 1999). Additionally, respiratory muscle fatigue and dyspnea have been observed in HCM during aerobic exertion (Arena et al., 2016).

It is important to select an appropriate animal model that closely resembles the human pathological profile. The R403Q mutation of the cardiac β-MyHC (MYH7) in rabbits is the closest phylogenetic model to the human MYH7 gene currently available (Lowey et al., 2018). Previously, the HCM mouse model has been used because it is easier to experimentally manipulate, and because they have myocyte disarray reminiscent of those seen in human disease (Geisterfer-Lowrance et al., 1996; Moore, Leinwand, & Warshaw, 2012). However, the adult mouse expresses only the α-MyHC isoform in the ventricle, which has evolved to optimize its power requirements for a small animal. Large mammals like rabbits and humans express predominantly the cardiac β-MyHC (Alpert et al., 2002; Malmqvist et al., 2004). The α and β-MyHC are sequentially 93% identical, and express similar phenotypes (Malmqvist et al., 2004), but have different mechanical characteristics.

The variation in human skeletal muscle fibers are primarily determined by the isoform of MyHC which are denoted as, slow I, fast IIA and fast IIX (Barnard, Edgerton, Furukawa, & Peter, 1971; Bottinelli & Reggiani, 2000; Brooke & Kaiser, 1970; Polla et al., 2004; Schiaffino & Reggiani, 1996). MyHC determines contractile properties in sarcomeres and convert the chemical energy of ATP into mechanical energy for muscle contraction (Bottinelli & Reggiani, 2000). It has been proven that the cardiac β-MyHC is expressed both in cardiac muscle and slow skeletal muscle (Tajsharghi & Fyhr, 2008). The human diaphragm and soleus muscle are predominantly composed

of slow oxidative or type I fibers (Gollnick et al., 1974; Lieberman et al., 1973; Maish, 2010; Mizuno, 1991; Sanchez et al., 1985; Widrick et al., 2001). The psoas muscle is composed mostly with fast-twitch fibers (Arbanas et al., 2009). It was expected that fast twitch muscle such as psoas does not change its activity in the rabbit model of HCM. These findings also indicate that the skeletal muscle weakness in R403Q rabbit model is associated with the muscle fiber types. A similar structural and sequential homology of class II myosin is present in cardiac and slow skeletal muscles. Hence, identical cardiac β-MyHC is expressed in these muscles (Lowey et al., 2018; Tajsharghi & Fyhr, 2008; Yu et al., 1993).

Microscopic examination of soleus muscle biopsies of HCM patients has shown a pattern that resembles a central core disease, which is a neuromuscular disorder associated with loss of mitochondria from the center of slow fibers (Fananapazir et al., 1993). This suggests that HCM mutations would have the same effect in both the human ventricle and slow skeletal muscle fibers. Histologically, subjects with dilated cardiomyopathy have been shown to exhibit abnormalities such as neonatal myosin staining and the presence of cores in diaphragm and quadriceps muscles, all of which suggest fiber type regeneration (Lindsay et al., 1996). This change in muscle structure is evident in the diaphragm of idiopathic dilated cardiomyopathy patients (Lindsay et al., 1996). Additionally, diaphragm muscle biopsies of HCM patients have been shown to fiber-type shift from fast glycolytic to slow oxidative fibers (Meyer et al., 2001; Tikunov et al., 1997). These histological abnormalities ultimately lead to diaphragm weakness, similar to what we found in this study.

We used the TG+ rabbit as a model, which has limitations but still provides insight on the contractile mechanisms of skeletal muscles in the presence of HCM mutations in the heart. Our finding that the actin velocity of sliding of the diaphragm in TG+ fibers is slower that in WT

muscles is consistent with previous clinical and histological evidence which shows that slow skeletal muscle weakness in associated with cardiomyopathy. This study adds substantial support for the hypothesis that HCM mutation plays a central role in weakening the slow twitch skeletal muscle fiber.

CHAPTER 3 - CONCLUSIONS AND FUTURE DIRECTIONS

Conclusions

In this thesis, we found that cardiomyopathy leads to loss of function of diaphragm and soleus muscle contractile proteins but it does not affect the psoas muscle at the molecular level. This is the first study that investigated the functional effect of both slow and fast skeletal muscles in the presence of the cardiac β-MyHC gene mutation which causes HCM. The reduced velocities of actin sliding and ATPase activity suggest that muscle weakness ultimately cause the functional defect of slow type I skeletal muscle can be attributed to the heart mutation. Altogether, these findings help us to understand the basic mechanism and functional effect of HCM on skeletal muscle.

Future directions

In the future, studies should be conducted with human samples, associated with extensive fiber typing, and mitochondrial functional analysis to elucidate the exact mechanism behind this slow skeletal muscle weakness. It would be important to investigate the expression of full-length cardiac myosin, location of the mutation and compare the effect of other types of mutation in order to conclude a unifying mechanism. This information could help us to understand new treatments for cardiomyopathy.

This thesis established that slow skeletal muscle is one of the expression sites of cardiomyopathy which might be useful in the future during the development of cardiomyopathy gene therapy. A fascinating future research project would be to investigate the effects of drugs to reverse the actin sliding velocity and ATPase activity on HCM. Such development could have a practical implication and could improve the quality of life of a cardiomyopathy patient by improving respiratory distress.

In moving forward, our laboratory has began looking into to contractile properties of diaphragm muscle in cardiomyopathy by measuring isometric force, force redevelopment, force enhancement, unloaded shortening velocity and calcium sensitivity at the myofibrils level. These measurement will give us an idea of the wide range of malfunction that happen during this condition.

REFERENCE

Alpert, N. R., Brosseau, C., Federico, A., Krenz, M., Robbins, J., & Warshaw, D. M. (2002). Molecular mechanics of mouse cardiac myosin isoforms. *Am J Physiol Heart Circ Physiol, 283*(4), H1446-1454. doi:10.1152/ajpheart.00274.2002

Arbanas, J., Klasan, G. S., Nikolic, M., Jerkovic, R., Miljanovic, I., & Malnar, D. (2009). Fibre type composition of the human psoas major muscle with regard to the level of its origin. *J Anat, 215*(6), 636-641. doi:10.1111/j.1469-7580.2009.01155.x

Arena, R., Lavie, C. J., Borghi-Silva, A., Daugherty, J., Bond, S., Phillips, S. A., & Guazzi, M. (2016). Exercise Training in Group 2 Pulmonary Hypertension: Which Intensity and What Modality. *Prog Cardiovasc Dis, 59*(1), 87-94. doi:10.1016/j.pcad.2015.11.005

Bahler, A. S., Fales, J. T., & Zierler, K. L. (1968). The dynamic properties of mammalian skeletal muscle. *J Gen Physiol, 51*(3), 369-384. doi:10.1085/jgp.51.3.369

Bales, A. C., & Sorrentino, M. J. (1997). Causes of congestive heart failure. Prompt diagnosis may affect prognosis. *Postgrad Med, 101*(1), 44-49, 54-46. doi:10.3810/pgm.1997.01.141

Bang, M. L., Centner, T., Fornoff, F., Geach, A. J., Gotthardt, M., McNabb, M., . . . Labeit, S. (2001). The complete gene sequence of titin, expression of an unusual approximately 700-kDa titin isoform, and its interaction with obscurin identify a novel Z-line to I-band linking system. *Circ Res, 89*(11), 1065-1072. doi:10.1161/hh2301.100981

Barnard, R. J., Edgerton, V. R., Furukawa, T., & Peter, J. B. (1971). Histochemical, biochemical, and contractile properties of red, white, and intermediate fibers. *Am J Physiol, 220*(2), 410-414. doi:10.1152/ajplegacy.1971.220.2.410

Barouch, W. W., & Moos, C. (1971). Effect of temperature on actin activation of heavy meromyosin ATPase. *Biochim Biophys Acta, 234*(2), 183-189. doi:10.1016/0005-2728(71)90073-9

Belus, A., Piroddi, N., Scellini, B., Tesi, C., D'Amati, G., Girolami, F., . . . Poggesi, C. (2008). The familial hypertrophic cardiomyopathy-associated myosin mutation R403Q accelerates tension generation and relaxation of human cardiac myofibrils. *J Physiol, 586*(15), 3639-3644. doi:10.1113/jphysiol.2008.155952

Bhagavan, N. V. (2002). Muscle and Nonmuscle Contractile Systems. In *Medical Biochemistry* (pp. 453-484): Elsevier.

Blank, S., Chen, V., & Ianuzzo, C. D. (1988). Biochemical characteristics of mammalian diaphragms. *Respir Physiol, 74*(1), 115-125.

Bolsterlee, B., Finni, T., D'Souza, A., Eguchi, J., Clarke, E. C., & Herbert, R. D. (2018). Three-dimensional architecture of the whole human soleus muscle in vivo. *PeerJ, 6*, e4610. doi:10.7717/peerj.4610

Bottinelli, R., & Reggiani, C. (2000). Human skeletal muscle fibres: molecular and functional diversity. *Prog Biophys Mol Biol, 73*(2-4), 195-262.

Brooke, M. H., & Kaiser, K. K. (1970). Muscle fiber types: how many and what kind? *Arch Neurol, 23*(4), 369-379.

Campbell, K. S., & Moss, R. L. (2002). History-dependent mechanical properties of permeabilized rat soleus muscle fibers. *Biophys J, 82*(2), 929-943. doi:10.1016/S0006-3495(02)75454-4

Cheng, Y. S., Matusovskiy, O. S., & Rassier, D. E. (2018). Cleavage of loops 1 and 2 in skeletal muscle heavy meromyosin (HMM) leads to a decreased function. *Arch Biochem Biophys, 661*, 168-177. doi:10.1016/j.abb.2018.11.002

Cirino, A. L., & Ho, C. (1993). Hypertrophic Cardiomyopathy Overview. In M. P. Adam, H. H. Ardinger, R. A. Pagon, S. E. Wallace, L. J. H. Bean, K. Stephens, & A. Amemiya (Eds.), *GeneReviews((R))*. Seattle (WA).

Colan, S. D., Lipshultz, S. E., Lowe, A. M., Sleeper, L. A., Messere, J., Cox, G. F., . . . Towbin, J. A. (2007). Epidemiology and cause-specific outcome of hypertrophic cardiomyopathy in children: findings from the Pediatric Cardiomyopathy Registry. *Circulation, 115*(6), 773-781. doi:10.1161/CIRCULATIONAHA.106.621185

Cuda, G., Fananapazir, L., Epstein, N. D., & Sellers, J. R. (1997). The in vitro motility activity of beta-cardiac myosin depends on the nature of the beta-myosin heavy chain gene mutation in hypertrophic cardiomyopathy. *J Muscle Res Cell Motil, 18*(3), 275-283.

Cuda, G., Fananapazir, L., Zhu, W. S., Sellers, J. R., & Epstein, N. D. (1993). Skeletal muscle expression and abnormal function of beta-myosin in hypertrophic cardiomyopathy. *J Clin Invest, 91*(6), 2861-2865. doi:10.1172/JCI116530

Dancker, P. (1975). ATPase activity and light scattering of acto-heavy meromyosin: dependence on ATP concentration and on ionic strength. *Z Naturforsch C, 30*(3), 379-384.

Darin, N., Tajsharghi, H., Ostman-Smith, I., Gilljam, T., & Oldfors, A. (2007). New skeletal myopathy and cardiomyopathy associated with a missense mutation in MYH7. *Neurology, 68*(23), 2041-2042. doi:10.1212/01.wnl.0000264430.55233.72

De Sousa, E., Veksler, V., Bigard, X., Mateo, P., Serrurier, B., & Ventura-Clapier, R. (2001). Dual influence of disease and increased load on diaphragm muscle in heart failure. *J Mol Cell Cardiol, 33*(4), 699-710. doi:10.1006/jmcc.2000.1336

Dominguez, J. F., & Howell, S. (2003). Compartmental analysis of steady-state diaphragm Ca2+ kinetics in chronic congestive heart failure. *Cell Calcium, 33*(3), 163-174.

Eddinger, T. J., & Moss, R. L. (1987). Mechanical properties of skinned single fibers of identified types from rat diaphragm. *Am J Physiol, 253*(2 Pt 1), C210-218. doi:10.1152/ajpcell.1987.253.2.C210

Eddinger, T. J., Moss, R. L., & Cassens, R. G. (1985). Fiber number and type composition in extensor digitorum longus, soleus, and diaphragm muscles with aging in Fisher 344 rats. *J Histochem Cytochem, 33*(10), 1033-1041. doi:10.1177/33.10.2931475

Edman, K. A. (1979). The velocity of unloaded shortening and its relation to sarcomere length and isometric force in vertebrate muscle fibres. *J Physiol, 291*, 143-159. doi:10.1113/jphysiol.1979.sp012804

Edman, K. A. (1988). Double-hyperbolic force-velocity relation in frog muscle fibres. *J Physiol, 404*, 301-321. doi:10.1113/jphysiol.1988.sp017291

Edman, K. A., & Hwang, J. C. (1977). The force-velocity relationship in vertebrate muscle fibres at varied tonicity of the extracellular medium. *J Physiol, 269*(2), 255-272. doi:10.1113/jphysiol.1977.sp011901

Edman, K. A., Reggiani, C., & te Kronnie, G. (1985). Differences in maximum velocity of shortening along single muscle fibres of the frog. *J Physiol, 365*, 147-163. doi:10.1113/jphysiol.1985.sp015764

Elliott, P. M., Anastasakis, A., Borger, M. A., Borggrefe, M., Cecchi, F., Charron, P., . . . Watkins, H. (2014). 2014 ESC Guidelines on diagnosis and management of hypertrophic cardiomyopathy: the Task Force for the Diagnosis and Management of Hypertrophic Cardiomyopathy of the European Society of Cardiology (ESC). *Eur Heart J, 35*(39), 2733-2779. doi:10.1093/eurheartj/ehu284

Fananapazir, L., Dalakas, M. C., Cyran, F., Cohn, G., & Epstein, N. D. (1993). Missense mutations in the beta-myosin heavy-chain gene cause central core disease in hypertrophic cardiomyopathy. *Proc Natl Acad Sci U S A, 90*(9), 3993-3997.

Fatkin, D., & Graham, R. M. (2002). Molecular mechanisms of inherited cardiomyopathies. *Physiol Rev, 82*(4), 945-980. doi:10.1152/physrev.00012.2002

Fatkin, D., McConnell, B. K., Mudd, J. O., Semsarian, C., Moskowitz, I. G., Schoen, F. J., . . . Seidman, J. G. (2000). An abnormal Ca(2+) response in mutant sarcomere protein-mediated familial hypertrophic cardiomyopathy. *J Clin Invest, 106*(11), 1351-1359. doi:10.1172/JCI11093

Fenn, W. O., & Marsh, B. S. (1935). Muscular force at different speeds of shortening. *J Physiol, 85*(3), 277-297. doi:10.1113/jphysiol.1935.sp003318

Ferreira, M., Santos-Silva, P. R., de Abreu, L. C., Valenti, V. E., Crispim, V., Imaizumi, C., . . . Ferreira, C. (2010). Sudden cardiac death athletes: a systematic review. *Sports Med Arthrosc Rehabil Ther Technol, 2*, 19. doi:10.1186/1758-2555-2-19

Fiorillo, C., Astrea, G., Savarese, M., Cassandrini, D., Brisca, G., Trucco, F., . . . Italian Network on Congenital, M. (2016). MYH7-related myopathies: clinical, histopathological and imaging findings in a cohort of Italian patients. *Orphanet J Rare Dis, 11*(1), 91. doi:10.1186/s13023-016-0476-1

Fonseca, S., Cachaldora, A., & Carballo, J. (2013). Characterization of Actin and Myosin Extracts Obtained Using Two Improved Laboratory Methods. *Food Analytical Methods*, *6*(4), 1033-1039. doi:10.1007/s12161-013-9654-0

Gehlbach, B. K., & Geppert, E. (2004). The pulmonary manifestations of left heart failure. *Chest, 125*(2), 669-682. doi:10.1378/chest.125.2.669

Geiger, P. C., Cody, M. J., Macken, R. L., & Sieck, G. C. (2000). Maximum specific force depends on myosin heavy chain content in rat diaphragm muscle fibers. *J Appl Physiol (1985), 89*(2), 695-703. doi:10.1152/jappl.2000.89.2.695

Geisterfer-Lowrance, A. A., Christe, M., Conner, D. A., Ingwall, J. S., Schoen, F. J., Seidman, C. E., & Seidman, J. G. (1996). A mouse model of familial hypertrophic cardiomyopathy. *Science, 272*(5262), 731-734.

Geisterfer-Lowrance, A. A., Kass, S., Tanigawa, G., Vosberg, H. P., McKenna, W., Seidman, C. E., & Seidman, J. G. (1990). A molecular basis for familial hypertrophic cardiomyopathy: a beta cardiac myosin heavy chain gene missense mutation. *Cell, 62*(5), 999-1006.

Gillis, T. E., Klaiman, J. M., Foster, A., Platt, M. J., Huber, J. S., Corso, M. Y., & Simpson, J. A. (2016). Dissecting the role of the myofilament in diaphragm dysfunction during the development of heart failure in mice. *Am J Physiol Heart Circ Physiol, 310*(5), H572-586. doi:10.1152/ajpheart.00773.2015

Glaser, J., & Suzuki, M. (2018). Skeletal Muscle Fiber Types in Neuromuscular Diseases. In K. Sakuma (Ed.), *Muscle Cell and Tissue - Current Status of Research Field*: InTech.

Gollnick, P. D., Sjodin, B., Karlsson, J., Jansson, E., & Saltin, B. (1974). Human soleus muscle: a comparison of fiber composition and enzyme activities with other leg muscles. *Pflugers Arch, 348*(3), 247-255.

Greaves, S. C., Roche, A. H., Neutze, J. M., Whitlock, R. M., & Veale, A. M. (1987). Inheritance of hypertrophic cardiomyopathy: a cross sectional and M mode echocardiographic study of 50 families. *Br Heart J, 58*(3), 259-266.

Hammond, M. D., Bauer, K. A., Sharp, J. T., & Rocha, R. D. (1990). Respiratory muscle strength in congestive heart failure. *Chest, 98*(5), 1091-1094.

Harvey, P. A., & Leinwand, L. A. (2011). The cell biology of disease: cellular mechanisms of cardiomyopathy. *J Cell Biol, 194*(3), 355-365. doi:10.1083/jcb.201101100

Hasenfuss, G. (1998). Animal models of human cardiovascular disease, heart failure and hypertrophy. *Cardiovasc Res, 39*(1), 60-76. doi:10.1016/s0008-6363(98)00110-2

Herman, I. M. (1993). Actin isoforms. *Curr Opin Cell Biol, 5*(1), 48-55.

Hilbert, L., Balassy, Z., Zitouni, N. B., Mackey, M. C., & Lauzon, A. M. (2015). Phosphate and ADP differently inhibit coordinated smooth muscle myosin groups. *Biophys J, 108*(3), 622-631. doi:10.1016/j.bpj.2014.12.008

Hilbert, L., Bates, G., Roman, H. N., Blumenthal, J. L., Zitouni, N. B., Sobieszek, A., . . . Lauzon, A. M. (2013). Molecular mechanical differences between isoforms of contractile actin in the presence of isoforms of smooth muscle tropomyosin. *PLoS Comput Biol, 9*(10), e1003273. doi:10.1371/journal.pcbi.1003273

Hill, A. V. (1938). The heat of shortening and the dynamic constants of muscle. *Proceedings of the Royal Society of London. Series B - Biological Sciences, 126*(843), 136-195. doi:10.1098/rspb.1938.0050

Ho, C. Y. (2010). Genetics and clinical destiny: improving care in hypertrophic cardiomyopathy. *Circulation, 122*(23), 2430-2440; discussion 2440. doi:10.1161/CIRCULATIONAHA.110.978924

Ho, C. Y., Day, S. M., Ashley, E. A., Michels, M., Pereira, A. C., Jacoby, D., . . . Olivotto, I. (2018). Genotype and Lifetime Burden of Disease in Hypertrophic Cardiomyopathy: Insights from the Sarcomeric Human Cardiomyopathy Registry (SHaRe). *Circulation, 138*(14), 1387-1398. doi:10.1161/CIRCULATIONAHA.117.033200

Ho, C. Y., Lopez, B., Coelho-Filho, O. R., Lakdawala, N. K., Cirino, A. L., Jarolim, P., . . . Seidman, C. E. (2010). Myocardial fibrosis as an early manifestation of hypertrophic cardiomyopathy. *N Engl J Med, 363*(6), 552-563. doi:10.1056/NEJMoa1002659

Ho, C. Y., & Seidman, C. E. (2006). A contemporary approach to hypertrophic cardiomyopathy. *Circulation, 113*(24), e858-862. doi:10.1161/CIRCULATIONAHA.105.591982

Hodge, K., Powers, S. K., Coombes, J., Fletcher, L., Demirel, H. A., Dodd, S. L., & Martin, D. (1997). Bioenergetic characteristics of the costal and crural diaphragm in mammals. *Respir Physiol, 109*(2), 149-154.

Holmes, K. C., & Geeves, M. A. (2000). The structural basis of muscle contraction. *Philos Trans R Soc Lond B Biol Sci, 355*(1396), 419-431. doi:10.1098/rstb.2000.0583

Homsher, E., Wang, F., & Sellers, J. R. (1992). Factors affecting movement of F-actin filaments propelled by skeletal muscle heavy meromyosin. *Am J Physiol, 262*(3 Pt 1), C714-723. doi:10.1152/ajpcell.1992.262.3.C714

Howard, J. (2001). *Mechanics of motor proteins and the cytoskeleton*. Sunderland, Mass.: Sinauer Associates, Publishers.

Howell, S., Maarek, J. M., Fournier, M., Sullivan, K., Zhan, W. Z., & Sieck, G. C. (1995). Congestive heart failure: differential adaptation of the diaphragm and latissimus dorsi. *J Appl Physiol (1985), 79*(2), 389-397. doi:10.1152/jappl.1995.79.2.389

Hughes, P. D., Polkey, M. I., Harrus, M. L., Coats, A. J., Moxham, J., & Green, M. (1999). Diaphragm strength in chronic heart failure. *Am J Respir Crit Care Med, 160*(2), 529-534. doi:10.1164/ajrccm.160.2.9810081

Huxley, A. F. (1957). Muscle structure and theories of contraction. *Prog Biophys Biophys Chem, 7*, 255-318.

Huxley, A. F. (2000). Mechanics and models of the myosin motor. *Philos Trans R Soc Lond B Biol Sci, 355*(1396), 433-440. doi:10.1098/rstb.2000.0584

Huxley, H. E. (1969). The mechanism of muscular contraction. *Science, 164*(3886), 1356-1365.

Jandreski, M. A., Sole, M. J., & Liew, C. C. (1987). Two different forms of beta myosin heavy chain are expressed in human striated muscle. *Hum Genet, 77*(2), 127-131. doi:10.1007/bf00272378

Jasmin, G., & Proschek, L. (1982). Hereditary polymyopathy and cardiomyopathy in the Syrian hamster. I. Progression of heart and skeletal muscle lesions in the UM-X7.1 line. *Muscle Nerve, 5*(1), 20-25. doi:10.1002/mus.880050105

Kalganov, A., Shalabi, N., Zitouni, N., Kachmar, L. H., Lauzon, A. M., & Rassier, D. E. (2013). Forces measured with micro-fabricated cantilevers during actomyosin interactions produced by filaments containing different myosin isoforms and loop 1 structures. *Biochim Biophys Acta, 1830*(3), 2710-2719.

Kasper, D. L. (2015). *Harrison's principles of internal medicine* (19th edition / editors, Dennis L. Kasper, MD, William Ellery Channing, Professor of Medicine, Professor of Microbiology, Department of Microbiology and Immunobiology, Harvard Medical School, Division of Infectious Diseases, Brigham and Women's Hospital, Boston, Massachusetts and five others . ed.). New York: McGraw Hill Education.

Kemp, G. J., Thompson, C. H., Stratton, J. R., Brunotte, F., Conway, M., Adamopoulos, S., . . . Rajagopalan, B. (1996). Abnormalities in exercising skeletal muscle in congestive heart failure can be explained in terms of decreased mitochondrial ATP synthesis, reduced metabolic efficiency, and increased glycogenolysis. *Heart, 76*(1), 35-41. doi:10.1136/hrt.76.1.35

Khaitlina, S. Y. (2015). Tropomyosin as a Regulator of Actin Dynamics. *Int Rev Cell Mol Biol, 318*, 255-291. doi:10.1016/bs.ircmb.2015.06.002

Ko, J. Y., Lee, M., Jang, J. H., Jang, D. H., & Ryu, J. S. (2019). A novel de novo mutation in MYH7 gene in a patient with early onset muscular weakness and severe kyphoscoliosis: A case report. *Medicine (Baltimore), 98*(28), e16389. doi:10.1097/MD.0000000000016389

Kolar, P., Neuwirth, J., Sanda, J., Suchanek, V., Svata, Z., Volejnik, J., & Pivec, M. (2009). Analysis of diaphragm movement during tidal breathing and during its activation while breath holding using MRI synchronized with spirometry. *Physiol Res, 58*(3), 383-392.

Kron, S. J., & Spudich, J. A. (1986). Fluorescent actin filaments move on myosin fixed to a glass surface. *Proc Natl Acad Sci U S A, 83*(17), 6272-6276. doi:10.1073/pnas.83.17.6272

Kron, S. J., Uyeda, T. Q., Warrick, H. M., & Spudich, J. A. (1991). An approach to reconstituting motility of single myosin molecules. *J.Cell Sci.Suppl, 14*, 129-133.

Labeit, S., Ottenheijm, C. A., & Granzier, H. (2011). Nebulin, a major player in muscle health and disease. *FASEB J, 25*(3), 822-829. doi:10.1096/fj.10-157412

Lai, A., Lichtwark, G. A., Schache, A. G., Lin, Y. C., Brown, N. A., & Pandy, M. G. (2015). In vivo behavior of the human soleus muscle with increasing walking and running speeds. *J Appl Physiol (1985), 118*(10), 1266-1275. doi:10.1152/japplphysiol.00128.2015

Lamont, P. J., Wallefeld, W., Hilton-Jones, D., Udd, B., Argov, Z., Barboi, A. C., . . . Laing, N. G. (2014). Novel mutations widen the phenotypic spectrum of slow skeletal/beta-cardiac myosin (MYH7) distal myopathy. *Hum Mutat, 35*(7), 868-879. doi:10.1002/humu.22553

Lauzon, A. M., Bates, J. H., Donovan, G., Tawhai, M., Sneyd, J., & Sanderson, M. J. (2012). A multi-scale approach to airway hyperresponsiveness: from molecule to organ. *Front Physiol, 3*, 191. doi:10.3389/fphys.2012.00191

Lavietes, M. H., Gerula, C. M., Fless, K. G., Cherniack, N. S., & Arora, R. R. (2004). Inspiratory muscle weakness in diastolic dysfunction. *Chest, 126*(3), 838-844. doi:10.1378/chest.126.3.838

Lecarpentier, Y., Chemla, D., Blanc, F. X., Pourny, J. C., Joseph, T., Riou, B., & Coirault, C. (1998). Mechanics, energetics, and crossbridge kinetics of rabbit diaphragm during congestive heart failure. *FASEB J, 12*(11), 981-989. doi:10.1096/fasebj.12.11.981

Lecarpentier, Y., Coirault, C., Langeron, O., Blanc, F. X., Salmeron, S., Attal, P., . . . Chemla, D. (1999). Impaired load dependence of diaphragm relaxation during congestive heart failure in the rabbit. *J Appl Physiol (1985), 87*(4), 1339-1345. doi:10.1152/jappl.1999.87.4.1339

Lecarpentier, Y., Coirault, C., Riou, B., Chemla, D., & Mercadier, J. J. (1999). Diaphragm strength and cross-bridge properties during chronic growth hormone hypersecretion. *Eur Respir J, 13*(5), 1070-1077.

Lehman, W., Craig, R., & Vibert, P. (1994). Ca(2+)-induced tropomyosin movement in Limulus thin filaments revealed by three-dimensional reconstruction. *Nature, 368*(6466), 65-67. doi:10.1038/368065a0

Lever, H. M., Karam, R. F., Currie, P. J., & Healy, B. P. (1989). Hypertrophic cardiomyopathy in the elderly. Distinctions from the young based on cardiac shape. *Circulation, 79*(3), 580-589.

Lewis, J. F., & Maron, B. J. (1989). Elderly patients with hypertrophic cardiomyopathy: a subset with distinctive left ventricular morphology and progressive clinical course late in life. *J Am Coll Cardiol, 13*(1), 36-45.

Lieber, R. L., Schmitz, M. C., Mishra, D. K., & Friden, J. (1994). Contractile and cellular remodeling in rabbit skeletal muscle after cyclic eccentric contractions. *J Appl Physiol (1985), 77*(4), 1926-1934. doi:10.1152/jappl.1994.77.4.1926

Lieberman, D. A., Faulkner, J. A., Craig, A. B., Jr., & Maxwell, L. C. (1973). Performance and histochemical composition of guinea pig and human diaphragm. *J Appl Physiol, 34*(2), 233-237. doi:10.1152/jappl.1973.34.2.233

Lindsay, D. C., Lovegrove, C. A., Dunn, M. J., Bennett, J. G., Pepper, J. R., Yacoub, M. H., & Poole-Wilson, P. A. (1996). Histological abnormalities of muscle from limb, thorax and diaphragm in chronic heart failure. *Eur Heart J, 17*(8), 1239-1250.

Lowey, S., Bretton, V., Joel, P. B., Trybus, K. M., Gulick, J., Robbins, J., . . . Rassier, D. E. (2018). Hypertrophic cardiomyopathy R403Q mutation in rabbit beta-myosin reduces contractile function at the molecular and myofibrillar levels. *Proc Natl Acad Sci U S A, 115*(44), 11238-11243. doi:10.1073/pnas.1802967115

Luther, P. K. (2009). The vertebrate muscle Z-disc: sarcomere anchor for structure and signalling. *J Muscle Res Cell Motil, 30*(5-6), 171-185. doi:10.1007/s10974-009-9189-6

Lymn, R. W., & Taylor, E. W. (1971). Mechanism of adenosine triphosphate hydrolysis by actomyosin. *Biochemistry, 10*(25), 4617-4624.

MacFarlane, N. G., Darnley, G. M., & Smith, G. L. (2000). Cellular basis for contractile dysfunction in the diaphragm from a rabbit infarct model of heart failure. *Am J Physiol Cell Physiol, 278*(4), C739-746. doi:10.1152/ajpcell.2000.278.4.C739

Maish, M. S. (2010). The diaphragm. *Surg Clin North Am, 90*(5), 955-968. doi:10.1016/j.suc.2010.07.005

Malinchik, S., Cuda, G., Podolsky, R. J., & Horowits, R. (1997). Isometric tension and mutant myosin heavy chain content in single skeletal myofibers from hypertrophic cardiomyopathy patients. *J Mol Cell Cardiol, 29*(2), 667-676. doi:10.1006/jmcc.1996.0309

Malmqvist, U. P., Aronshtam, A., & Lowey, S. (2004). Cardiac myosin isoforms from different species have unique enzymatic and mechanical properties. *Biochemistry, 43*(47), 15058-15065. doi:10.1021/bi0495329

Mancini, D. M., Ferraro, N., Nazzaro, D., Chance, B., & Wilson, J. R. (1991). Respiratory muscle deoxygenation during exercise in patients with heart failure demonstrated with near-infrared spectroscopy. *J Am Coll Cardiol, 18*(2), 492-498. doi:10.1016/0735-1097(91)90605-9

Mancini, D. M., Henson, D., LaManca, J., & Levine, S. (1992). Respiratory muscle function and dyspnea in patients with chronic congestive heart failure. *Circulation, 86*(3), 909-918. doi:10.1161/01.cir.86.3.909

Marian, A. J. (2011). Modeling human disease phenotype in model organisms: "It's only a model!". *Circ Res, 109*(4), 356-359. doi:10.1161/CIRCRESAHA.111.249409

Marian, A. J., Wu, Y., Lim, D. S., McCluggage, M., Youker, K., Yu, Q. T., . . . Roberts, R. (1999). A transgenic rabbit model for human hypertrophic cardiomyopathy. *J Clin Invest, 104*(12), 1683-1692. doi:10.1172/JCI7956

Maron, B. J. (2002). Hypertrophic cardiomyopathy: a systematic review. *JAMA, 287*(10), 1308-1320.

Matusovsky, O. S., Mansson, A., Persson, M., Cheng, Y. S., & Rassier, D. E. (2019). High-speed AFM reveals subsecond dynamics of cardiac thin filaments upon Ca(2+) activation and heavy meromyosin binding. *Proc Natl Acad Sci U S A*. doi:10.1073/pnas.1903228116

Matusovsky, O. S., Shevchenko, U. V., Matusovskaya, G. G., Sobieszek, A., Dobrzhanskaya, A. V., & Shelud'ko, N. S. (2015). Catch Muscle Myorod Modulates ATPase Activity of Myosin in a Phosphorylation-Dependent Way. *PLoS One, 10*(4). doi:ARTN e0125379 10.1371/journal.pone.0125379

McNally, E. M., & Goldstein, J. A. (2012). Interplay between heart and skeletal muscle disease in heart failure: the 2011 George E. Brown Memorial Lecture. *Circ Res, 110*(5), 749-754. doi:10.1161/CIRCRESAHA.111.256776

Mescher, A. L., & Junqueira, L. C. U. (2016). *Junqueira's basic histology: text and atlas* (F. edition Ed.). New York Chicago San Francisco: McGraw Hill Education.

Meyer, F. J., Borst, M. M., Zugck, C., Kirschke, A., Schellberg, D., Kubler, W., & Haass, M. (2001). Respiratory muscle dysfunction in congestive heart failure: clinical correlation and prognostic significance. *Circulation, 103*(17), 2153-2158.

Minozzo, F. C., & Rassier, D. E. (2010). Effects of blebbistatin and Ca2+ concentration on force produced during stretch of skeletal muscle fibers. *Am J Physiol Cell Physiol, 299*(5), C1127-1135. doi:10.1152/ajpcell.00073.2010

Mizuno, M. (1991). Human respiratory muscles: fibre morphology and capillary supply. *Eur Respir J, 4*(5), 587-601.

Moore, J. R., Leinwand, L., & Warshaw, D. M. (2012). Understanding cardiomyopathy phenotypes based on the functional impact of mutations in the myosin motor. *Circ Res, 111*(3), 375-385. doi:10.1161/CIRCRESAHA.110.223842

Niimura, H., Bachinski, L. L., Sangwatanaroj, S., Watkins, H., Chudley, A. E., McKenna, W., . . . Seidman, C. E. (1998). Mutations in the gene for cardiac myosin-binding protein C and

late-onset familial hypertrophic cardiomyopathy. *N Engl J Med, 338*(18), 1248-1257. doi:10.1056/NEJM199804303381802

Nishimura, R. A., Ommen, S. R., & Tajik, A. J. (2003). Cardiology patient page. Hypertrophic cardiomyopathy: a patient perspective. *Circulation, 108*(19), e133-135. doi:10.1161/01.CIR.0000097621.97566.96

Palmiter, K. A., Tyska, M. J., Haeberle, J. R., Alpert, N. R., Fananapazir, L., & Warshaw, D. M. (2000). R403Q and L908V mutant beta-cardiac myosin from patients with familial hypertrophic cardiomyopathy exhibit enhanced mechanical performance at the single molecule level. *J Muscle Res Cell Motil, 21*(7), 609-620.

Polla, B., D'Antona, G., Bottinelli, R., & Reggiani, C. (2004). Respiratory muscle fibres: specialisation and plasticity. *Thorax, 59*(9), 808-817. doi:10.1136/thx.2003.009894

Ralston, S. H., Penman, I. D., Strachan, M. W., & Hobson, R. P. (2018). *Davidson's principles and practice of medicine*.

Rassier, D. E. (2010). *Muscle biophysics : from molecules to cells*. New York: Springer.

Rayment, I. (1996). The structural basis of the myosin ATPase activity. *J Biol Chem, 271*(27), 15850-15853.

Rayment, I., Holden, H. M., Whittaker, M., Yohn, C. B., Lorenz, M., Holmes, K. C., & Milligan, R. A. (1993). Structure of the actin-myosin complex and its implications for muscle contraction. *Science, 261*(5117), 58-65.

Ribeiro, J. P., Chiappa, G. R., Neder, J. A., & Frankenstein, L. (2009). Respiratory muscle function and exercise intolerance in heart failure. *Curr Heart Fail Rep, 6*(2), 95-101.

Ribeiro, P. A., Ribeiro, J. P., Minozzo, F. C., Pavlov, I., Leu, N. A., Kurosaka, S., . . . Rassier, D. E. (2013). Contractility of myofibrils from the heart and diaphragm muscles measured with

atomic force cantilevers: effects of heart-specific deletion of arginyl-tRNA-protein transferase. *Int J Cardiol, 168*(4), 3564-3571. doi:10.1016/j.ijcard.2013.05.069

Sanchez, J., Medrano, G., Debesse, B., Riquet, M., & Derenne, J. P. (1985). Muscle fibre types in costal and crural diaphragm in normal men and in patients with moderate chronic respiratory disease. *Bull Eur Physiopathol Respir, 21*(4), 351-356.

Schiaffino, S., & Reggiani, C. (1996). Molecular diversity of myofibrillar proteins: gene regulation and functional significance. *Physiol Rev, 76*(2), 371-423. doi:10.1152/physrev.1996.76.2.371

Shelud'ko, N. S., Matusovsky, O. S., Permyakova, T. V., & Matusovskaya, G. G. (2007). "Twitchin-actin linkage hypothesis" for the catch mechanism in molluscan muscles: evidence that twitchin interacts with myosin, myorod, and paramyosin core and affects properties of actomyosin. *Arch Biochem Biophys, 466*(1), 125-135. doi:10.1016/j.abb.2007.07.014

Siccardi, M. A., & Valle, C. (2018). Anatomy, Bony Pelvis and Lower Limb, Psoas Major. In *StatPearls*. Treasure Island (FL).

Spudich, J. A. (2014). Hypertrophic and dilated cardiomyopathy: four decades of basic research on muscle lead to potential therapeutic approaches to these devastating genetic diseases. *Biophys J, 106*(6), 1236-1249. doi:10.1016/j.bpj.2014.02.011

Staron, R. S. (1997). Human skeletal muscle fiber types: delineation, development, and distribution. *Can J Appl Physiol, 22*(4), 307-327.

Stassijns, G., Gayan-Ramirez, G., De Leyn, P., de Bock, V., Dom, R., Lysens, R., & Decramer, M. (1999). Effects of dilated cardiomyopathy on the diaphragm in the Syrian hamster. *Eur Respir J, 13*(2), 391-397.

Supinski, G., DiMarco, A., & Dibner-Dunlap, M. (1994). Alterations in diaphragm strength and fatiguability in congestive heart failure. *J Appl Physiol (1985), 76*(6), 2707-2713. doi:10.1152/jappl.1994.76.6.2707

Sweeney, H. L., & Houdusse, A. (2010). Structural and functional insights into the Myosin motor mechanism. *Annu Rev Biophys, 39*, 539-557. doi:10.1146/annurev.biophys.050708.133751

Szent-Gyorgyi, A. G. (2004). The early history of the biochemistry of muscle contraction. *J Gen Physiol, 123*(6), 631-641. doi:10.1085/jgp.200409091

Tajsharghi, H., & Fyhr, I. M. (2008). Structural effects of the slow/b-cardiac myosin heavy chain R453C mutation in cardiac and skeletal muscle. *Scand Cardiovasc J, 42*(2), 153-156. doi:10.1080/14017430701762701

Tang, W., Blair, C. A., Walton, S. D., Malnasi-Csizmadia, A., Campbell, K. S., & Yengo, C. M. (2016). Modulating Beta-Cardiac Myosin Function at the Molecular and Tissue Levels. *Front Physiol, 7*, 659. doi:10.3389/fphys.2016.00659

Tikunov, B., Levine, S., & Mancini, D. (1997). Chronic congestive heart failure elicits adaptations of endurance exercise in diaphragmatic muscle. *Circulation, 95*(4), 910-916.

van der Velden, J., & Stienen, G. J. M. (2019). Cardiac Disorders and Pathophysiology of Sarcomeric Proteins. *Physiol Rev, 99*(1), 381-426. doi:10.1152/physrev.00040.2017

van Hees, H. W., van der Heijden, H. F., Hafmans, T., Ennen, L., Heunks, L. M., Verheugt, F. W., & Dekhuijzen, P. N. (2008). Impaired isotonic contractility and structural abnormalities in the diaphragm of congestive heart failure rats. *Int J Cardiol, 128*(3), 326-335. doi:10.1016/j.ijcard.2007.06.080

van Hees, H. W., van der Heijden, H. F., Ottenheijm, C. A., Heunks, L. M., Pigmans, C. J., Verheugt, F. W., . . . Dekhuijzen, P. N. (2007). Diaphragm single-fiber weakness and loss of myosin in congestive heart failure rats. *Am J Physiol Heart Circ Physiol, 293*(1), H819-828. doi:10.1152/ajpheart.00085.2007

Warshaw, D. M. (2004). Lever arms and necks: a common mechanistic theme across the myosin superfamily. *J Muscle Res Cell Motil, 25*(6), 467-474. doi:10.1007/s10974-004-1767-z

Widrick, J. J., Romatowski, J. G., Norenberg, K. M., Knuth, S. T., Bain, J. L., Riley, D. A., . . . Fitts, R. H. (2001). Functional properties of slow and fast gastrocnemius muscle fibers after a 17-day spaceflight. *J Appl Physiol (1985), 90*(6), 2203-2211. doi:10.1152/jappl.2001.90.6.2203

Wigle, E. D., Rakowski, H., Kimball, B. P., & Williams, W. G. (1995). Hypertrophic cardiomyopathy. Clinical spectrum and treatment. *Circulation, 92*(7), 1680-1692.

Witt, C., Borges, A. C., Haake, H., Reindl, I., Kleber, F. X., & Baumann, G. (1997). Respiratory muscle weakness and normal ventilatory drive in dilative cardiomyopathy. *Eur Heart J, 18*(8), 1322-1328.

Yu, Q. T., Ifegwu, J., Marian, A. J., Mares, A., Jr., Hill, R., Perryman, M. B., . . . Roberts, R. (1993). Hypertrophic cardiomyopathy mutation is expressed in messenger RNA of skeletal as well as cardiac muscle. *Circulation, 87*(2), 406-412.

Yutaka, Y., Omasa, M., Matsumoto, M., Ueda, Y., Tomiyama, K., Shikuma, K., . . . Taki, T. (2010). [A case of complete resection of a squamous cell lung cancer invading diaphragm after neoadjuvant chemotherapy of nedaplatin and irinotecan]. *Gan To Kagaku Ryoho, 37*(11), 2151-2153.

Zhu, E., Petrof, B. J., Gea, J., Comtois, N., & Grassino, A. E. (1997). Diaphragm muscle fiber injury after inspiratory resistive breathing. *Am J Respir Crit Care Med, 155*(3), 1110-1116. doi:10.1164/ajrccm.155.3.9116995